Acknowledgments

The experimental process of this thesis has been conducted in the Chemosensory lab, at the Neuroscience Unit of the Department of Psychology, at the Norwegian University of Science and Technology (NTNU). The writing of this thesis has been completed at the Department of Neuroscience, NTNU.

I would like to express my thanks to my main supervisor, Professor Bente Gunnveig Berg, for accepting me into her lab, and giving me the opportunity to successfully complete my masters thesis. I would also like to thank her for taking the time and care to read through my thesis, providing invaluable feedback. To Elena Ian, my second supervisor, I would like to extend my gratitude, for teaching me the experimental procedures, and for her guidance during the experimental period, as well as for providing helpful feedback after reading my thesis. I am particularly grateful for the assistance provided by Nicholas Kirkerud, whilst showing remarkable patience, during the data analysis period. In addition to those noted above, I wish to acknowledge Hanna Mustaparta, as well as my fellow students Andreas Lande and Ida Kjos, for making the time spent in the lab here during the past year an enjoyable, knowledgeable experience.

Abstract

Herbivorous insects as model organisms have been shown to be very useful in studies related to neuronal and molecular elements of the olfactory system, and for studying the mechanisms of olfactory coding. Naturally occurring stimuli are usually presented as mixtures of numerous single odours. In the study presented here, calcium imaging of odour-evoked responses in the antennal lobe (AL) of the heliothine moth was conducted during stimulation with single plant odours and ternary mixtures, composed of a binary pheromone mixture and a single plant odour. Prior to the calcium imaging measurement, projection neurons were stained, with fura-dextran, via retrograde transportation after injection into the calyces of the mushroom body. Time traces of AL glomeruli from different individuals showed that the strongest responding glomeruli were all located within close proximity to each other. An overall suppressive effect of pheromones on plant odour evoked responses in the AL was identified when using ternary stimuli, with a few cases of synergistic effects of plant odours on pheromone-evoked responses being found. In addition, it was shown that the responses in the macroglomerular complex were greater when stimulating with the pheromone mixture than with the primary pheromone component alone.

Table of Contents

1. Introduction

Humans − a species considerably visually orientated − often find it difficult to comprehend the importance of chemical sensitivity to life. Chemo-sensation, however, can be observed within all living organisms including the simplest of lifeforms, such as bacteria, protozoans, and slime moulds. Actually, every living cell is reactive to chemicals in one way or another, and this sensitivity is what most likely led to the evolutionary development of specific receptor proteins for the detection of external chemical signals, and finally to the specific chemosensory organs and olfactory systems that can be observed today (Ache and Young, 2005). Animals are dependent on their senses. Their sensory system is what provides the information required in the nervous system to create a simplified internal representation of the complex external world, whereby animals are able to perform the correct behavioural responses in various situations (Hansson and Stensmyr, 2011). As noted above, over the course of evolution, animals (vertebrates and insects in particular) have developed a complex array of chemosensory receptors that are used to detect and distinguish different odours (Kaupp, 2010). The ability to detect and respond in an adaptive manner to chemical signals serves as the primary window to the sensory world for most species of animals (Ache and Young, 2005). The location and avoidance of predators as well as the location and assessment of food, shelter, mates, and breeding substrates can be dependent on the olfactory system. As such, one could argue that the survival and reproduction of the vast majority of animal species is underpinned by olfaction. Yet, compared to the progress made and knowledge ascertained regarding the other sensory systems, olfactory coding and perception is still a long way from being understood (Galizia and Rössler, 2010; Hansson and Stensmyr, 2011).

1.1. *Insects as model organisms*

Herbivorous insects as model organisms have been shown to be very useful in studies related to neuronal and molecular elements of the olfactory system, and for studying the mechanisms of olfactory coding, due to their varied and unique ability to adapt to their host plants which can be located and selected using chemical cues (Mustapata, 2002). The role of odours in the life of an insect is pivotal. Research conducted since the 1950's until very recently, regarding insect olfactory structure and function, has quite often preceded comparable investigations in vertebrates, as well as having been significant during the formulation of general principles (Hansson, 2002).

Thanks to their easily accessible and simple nervous systems possessing few and readily identifiable cells, many principle olfactory coding mechanisms in the brain have been documented, supporting their usage as an effective alternative to the complex nervous systems of vertebrates (Rø *et al*, 2007). As well as their ease of accessibility, there is also recurring similarities between the insect and vertebrate parallel olfactory subsystems, further reinforcing the importance of having this model organism available to us (Galizia and Rössler, 2010)

It has been shown in all organisms that have an olfactory system that their olfactory sensory neurons (OSNs) project directly to the central nervous system (CNS) with their axons terminating in the antennal lobe (AL) in insects, and olfactory bulb (OB) in vertebrates which both comprise of spherical structures known as glomeruli (Hansson, 2002). Moreover, the expansion of neuroscientific studies beyond the already established laboratory models is of great importance to help verify the generality of processes and functions (Hansson and Stensmyr, 2011).

1.2. *Moths as a model insect for research on olfactory processing*

Among the vast numbers of insect species available to us for study, the moth is one of the most widely used. These noctuid organisms are a desired choice for research as a result of their extreme sensitivity and species specific pheromone system, as well as their predictable pheromone induced behaviours, and the dimensions of their antennae (Sachse and Krieger, 2011). Of all the moths that have been utilised in research, a commonly used and most in depth studied is a small number of the monophyletic subfamily Heliothinae (Lepidoptera: Notuidae), which is comprised of approximately 365 diverse species located on five of the seven continents in warm, dry regions (Cho *et al*, 2008; Berg *et al*, 2014)

These moths are of particular interest due to the female produced compounds for communication of sympatric species occurring within and across the different species. And so the males of these species characteristically have an olfactory system that is comprised of two functionally distinct arrangements: one that carries the information from pheromones used for their attraction, and the other to signal information arising from heterospecifics, which makes certain that the male targets the conspecific female (Berg *et al*, 2014).

As well as this fascinating arrangement, another reason for the use and study of the heliothine moth olfactory system is due to their notoriety as one of the world's most destructive crop pests that amounts to billions of dollars annually. This calls for the creation of alternative

forms of defence against these pests through the development of species-specific control techniques using pheromones, as opposed to traditional insecticides. (Almaas and Mustaparta, 1990; Cho *et al,* 2008; Sachse and Krieger, 2011; Berg *et al*, 2014)

1.3. *Anatomy of the moth olfactory system*

1.3.1. Peripheral organization

Of all the senses that insects possess, the sense of smell is arguable the most important, as has been noted above. This importance can be represented in the various intricate antennal structures (the functional equivalents of the human nose) found across insect species (Hansson and Stensmyr, 2011). Moths have evolutionarily developed the ability to communicate through the detection of chemical signals in the form of pheromones emitted by females, over distances that can reach more than a kilometre. Moths are able to detect these chemical signals due to the hair like structures located on the antennae known as sensilla. Sensilla differ in their morphological shape, the long trichoid sensilla are ideal for the creation of basket-type sieves, which are used (in males) for the detection of the female produced pheromones. Amongst the long trichoid sensilla there are also shorter sensilla that can be found in a high density. These sensilla are responsible for the detection of plant odours (Steinbrecht *et al,* 1995; Galizia and Rössler, 2010). As well as pheromone detection, male moths are also able to distinguish plant and food odours, which has given rise to a subdivision of the olfactory system (Mustaparta, 1996; Berg *et al*, 2014).

Within each antennal segment, along the whole antennae, OSNs are compartmentalised according the olfactory sensilla. In moths, individual sensilla typically house two to four OSNs. Each sensory neuron carries odour receptors, which are heteromeric ligand gated ion channels comprised of heteromeric complexes. Within the sensillum lymph, olfactory binding proteins (OBPs) bind plant odours as well as pheromones, carrying the ligand through the sensillum to the odour receptor (Almaas and Mustaparta, 1991; Mustaparta, 1996; Berg *et al*, 2002; Hillier *et al,* 2006; Sato *et al,* 2008; Galizia and Rössler, 2010; Suh *et al*, 2014). From here the OSNs carrying the olfactory information project directly to the primary olfactory centre, the AL. Males of the *Heliothis virescens* species have developed a male-specific pathway that carries information of four female-produced substances that are detected by four physiological types of sensory neurons (Berg *et al*, 1998).

1.3.2. The primary olfactory centre of the brain, the antennal lobe (AL)

The OSNs arriving from the antenna terminate in the AL of the moth on neuropil of spheroidal structures called glomeruli. Each glomerulus seems to have a specialised perception of particular odours due to the OSNs that express the same type of odour receptor terminating on the neuropil, creating odortypic regions. This type of organization functions in parallel with the "odotopic" odour maps described in the OB in mammals (Berg *et al,* 2002; 2014).The total number of glomeruli in moths, including dimorphic and isomorphic units, comprises ~80 glomeruli (recently identified in the male *Helicoverpa armigera* by Zhao *et al,* 2016). Generally, the glomerulus has been defined as "a synaptic complex enclosed in glial membranes or otherwise set apart" by Shepherd (1974). These are arranged by having one centrally located unit called the cumulus, surrounded by three satellite glomeruli, which are located dorsally in the AL at the entrance of the antennal nerve (Berg *et al,* 2002).

The OSNs conveying information about pheromones project to a group of specialised sexually dimorphic glomeruli called the macroglomerular complex (MGC), at the entrance of the antennal nerve in the AL, whereas the OSNs containing information about the plant odours project to ordinary glomeruli. Here, in the AL, the formation of the first relay for processing odour information takes place (Mustaparta, 1996; Berg *et al,* 2002; Hillier *et al,* 2006; Berg *et al,* 2002). It has been shown in *Heliothis virescens* that the receptor neuron types that detect female produced substances (which have been identified) amounts to the same number of glomeruli that forms the MGC (the male specific pathway noted above projecting to four MGC compartments), and the way the MGC is organised assists in the processing of pheromones of closely related species, in order to avoid cross attraction (Hillier *et al,* 2006).

It has been demonstrated in a number of insect species (Homberg *et al*. 1989) that the glomeruli are innervated by neurites of two main types of antennal lobe neurons: : 1) the local interneurons (LNs), which remain in the AL communicating within it, and 2) the projection neurons (PNs), which send axons to higher integration centres in the protocerebrum. A third and minor type of antennal-lobe neurons includes the centrifugal neurons, who have dendritic arborisations outside the AL, and send axons into the AL (Rø *et al*, 2007; Homberg *et al,* 1989; Berg *et al,* 2007; 2014).

1.3.3. Local interneurons (LNs)

Within the AL, the glomeruli are connected together by a large network of mostly GABAergic LNs (Hoskins et al. 1984; Berg et al. 2009). These neurons have abundant branches, and may extend processes into all glomeruli of the AL (Christensen *et al,* 2001; Reisenman *et al,* 2011). The LNs deal out their inhibitory effects throughout the AL due to their characteristically wide field organisation. This arrangement allows the global modulation of output in the whole glomerular array (Christensen *et al,* 2001). There have been numerous different morphological types of LNs described in several species of insects, with ~360 extensive arborisations being recorded in *M. sexta* that overlap spatially with antennal receptor axonal projections and arborisations of PNs (Christensen *et al,* 1993). The GABAergic LNs are the primary source of inhibition of the PNs, which go through complex responses of excitation and inhibition when having been stimulated with odours, and are thought to shape the patterns of activity of the glomeruli when evoked by olfactory stimuli (Christensen *et al,* 2001).

1.3.4. Projection neurons (PNs)

PNs seem to be highly conserved in their morphological appearance, have dendritic ramifications in the AL, and function to send their axons containing olfactory information from the AL to higher integration centres in the protocerebrum via the three main antennal lobe tracts (ALTs) (figure 1). These pathways are now known as the medial ALT (mALT), mediolateral ALT (mlALT), and the lateral ALT (lALT), which were formerly known as the inner antenno-cerebral tract (iACT), middle antenno-cerebral tract (mACT), and outer antenno-cerebral tract (oACT) respectively (Homberg *et al,* 1989; Kanzaki *et al,* 1989; Berg *et al,* 2007; Ito *et al,* 2014). Studies using Lepidoptera have revealed two additional ALTs: a dorsal and a dorso-medial ALT (Homber *et al,* 1988; Schachtner *et al,* 2005). Uniglomerular PNs (uPNs) within the mALT, the most prominent tract, send their axons to the calyces of the mushroom bodies (MB) and to areas in the lateral protocerebrum, called the lateral horn. The mlALT and lALT, on the other hand, send their axons directly to the lateral horn (Boeckh and Ernst, 1987; Kanzaki *et al,* 2003; Schachtner *et al,* 2005; Zhao *et al,* 2014). The uniglomerular PNs within the mALT form synapses with MB Kenyon cells (KCs), which form MB lobes and create distinct layers, and the calyses of the MB have been found to be essential for olfactory learning and short term memory in odour discrimination tasks (Heisenberg, 1998; Galizia and Rössler, 2010). The PNs that have been the most comprehensively studied are the uPNs confined to the mALT. These PNs are characterised by

being contained to a single glomerulus in the AL. In a study by Sun et al (1997) it was shown that each PN possessed a cell body within one of three cell body clusters of the AL, a primary neurite extending over the coarse neuropil at the centre of the AL, and a single axon stemming from the primary neurite which projects to the calyces of the MB before terminating in the lateral horn of the ipsilateral protocerebrum.

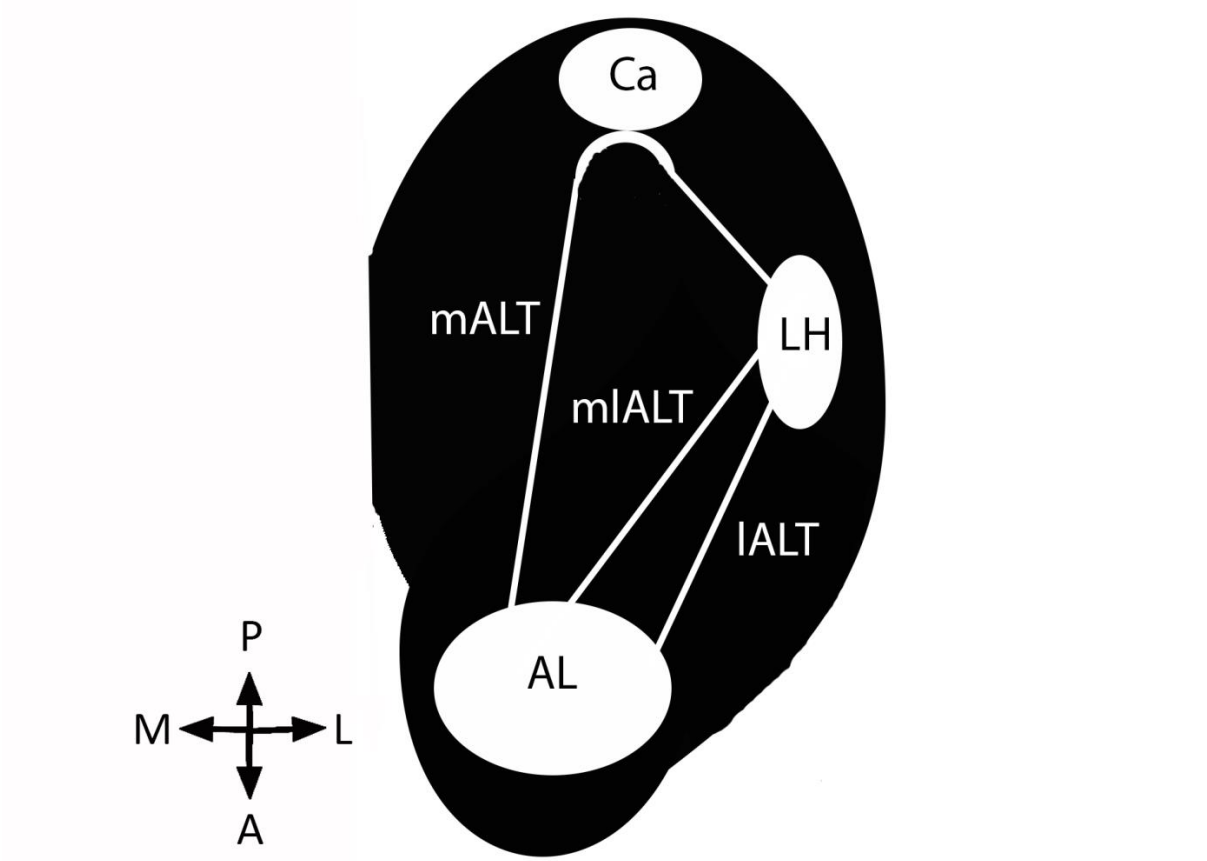

Figure 1: Schematic display of one heliothine moth brain hemisphere. Ca Calyses, LH Lateral horn, AL Antennal lobe, mALT medial antennal lobe tract (ALT), mlALT mediolateral ALT, lALT lateral ALT. Orientation indicated (A = anterior, M = medial, P = posterior, L = lateral).

1.3.5. Centrifugal neurons

Centrifugal neurons appear to possess feedback properties, and have dendritic ramifications in other parts of the nervous system, as well as multiglomerular ramification in both ALs (Homberg *et al*, 1989). These neurons often have a prominent soma outside the AL neuropil. These neurons exist in small numbers, the most common in insects being midline neurons of the suboesophageal ganglion (SEG) with ascending axonal projections to both ALs, (Homberg *et al*, 1989)

1.3.6. Neurotransmitters of the moth brain

Within the brain and peripheral nervous system of insects, a number of different neurotransmitters have been identified. There have been various studies reporting acetylcholine as the primary transmitter of OSNs and some of the PNs (reviewed by Schachtner et al. 2005). Moreover, a large number of GABAergic AL LNs has been found in all insect species that have been studied to date (Schachtner *et al,* 2005). Also, the insect nervous system utilizes biogenic amines as neurotransmitters: serotonin-ir fibres innervate all AL glomeruli, dopamine has been confined in the AL, octopamine-ir fibres have been shown to give rise to blebbed arborisations that ascend through circumoesophageal connectives, and histamine may act as a second inhibitory transmitter at ORNs and PNs (Schachtner *et al,* 2005). Neuropeptides have also been reported to play a role in the olfactory system of insects. The most common neuropeptide families include: the A-type allatostatins (ASTAs), the allototropins (Ats), the FMRFamide-related peptides (FaRPs), and tachykinin related peptides (TKRPs) (Schachtner *et al,* 2005; Berg *et al,* 2007).

1.4. *Physiological responses of individual neurons*

The insect pheromone olfactory system has become a model, as a result of its simplicity and well documented chemical signalling and neuronal pathways, to understand how the more complex plant odour information is encoded. Within the pheromone olfactory system a number of OSN types have been recognised in heliothine moths, that share the same major pheromone component, with each neuron responding to one compound (Almaas & Mustaparta, 1990;1991; Berg & Mustaparta 1995). A tip recording study with staining conducted by Berg *et al* (1998) revealed how neurons are able to converge in the AL and mediate olfactory information to central neurons, and in heliothine moths it has been documented one glomerular unit in the MGC receives input from one type of OSN (Mustaparta, 2002).

Identifying the complex blends of plant volatiles as cues to locate and select a host, in insects, has become a challenge when studying insect-plant interactions. To overcome this, the plant odour olfactory system in heliothine moths has been investigated and compared, by identifying biologically relevant odours using combined gas chromatography with electrophysiological recording from single OSNs (Mustaparta, 2002). 17 different types of plant OSNs have been discovered, after having tested a number of plant volatiles as mixtures, as well as the identification of a major neuron type in 80% of the recordings from heliothine

moths. These neurons show high selectivity and sensitivity when using doses as low as picograms in experiments (Røstelien *et al*, 2000) Results obtained from Schmidt *et al* (1998), Mozuraitis *et al* (2002), and Stranden *et al* (2002) have revealed that heliothine plant OSNs are as finely tuned as the pheromone OSNs, and that there is no overlap of responses from the identified plant OSNs.

1.5. *Calcium imaging*

Electrophysiology has been in use since the mid-20th century, with numerous studies including insects. Different electrophysiological techniques have been developed since the electroantennogram (EAG) in 1957, including the introduction of single cell recordings (SCR), and the patch clamp technique. These techniques have allowed measurement of voltage output in the antennae of insects to the brain, the recording of action potentials (AP) in single olfactory neurons, the study of single or multiple ion channels in cells, and characterization of general coding principles characterizing the olfactory pathways (Calatayud, 2014). One of the insect species most intensively studied by the single cell recording technique is the moth *H. virescens.* Thus, odor-evoked response patterns of individual neurons at different levels of the olfactory pathway including OSNs (Berg *et al*, 1995; 1998; Røstelien *et al*, 2000a; 2000b; Berg *et al*, 2005; Baker *et al*, 2004) and PNs (Christensen et al. 1995; Vickers et al. 1998; Zhao et al. 2014) have been particularly well described in this species. The introduction of a new class of voltage sensitive dyes, which created the possibility of being able to optically image neuronal circuits at whole brain level, led to the development of calcium sensitive dyes and has thus provided an invaluable optical method for studying information processing in whole neural networks. Especially when used in tandem with two photon laser scanning microscopy (Calatayud, 2014).

Measuring neuronal activity in undisturbed nervous tissue through the use of calcium imaging, by exploiting intrinsic changes in tissue properties, has become a more widely used and important tool to study the brain of insects (Galizia *et al*, 1997). Calcium ions generate versatile intracellular signals that determine a large variety of functions in virtually every cell type in biological organisms (Grienberger and Konnerth, 2012). A critical breakthrough in calcium imaging came in the synthesis of new, more sensitive fluorescent indicators such as Fura-2, deposing its predecessor ‘quina’, and offered up to 30–fold brighter fluorescence, with longer wavelengths of excitation (350-380nm), and a greater selectivity for calcium over other divalent cations. Fura-2 is of particular use as it permits quantitative calcium

measurements which involves using the ratios of the signals obtained from alternating the excitation of wavelengths (Grynkiewicz *et al*, 1985; Grienberger and Konnerth 2012).

Our knowledge of odour representations of neural circuits in the AL of insects has greatly improved as a direct result of the development of optical imaging techniques, such as calcium imaging, which permits repeated measurement of summated odour evoked activity in a population of neurons, in a number of glomeruli at the same time, as well as allowing the visualisation of odour evoked activity patterns with good spatial and reasonable temporal resolution (Lieke, 1993; Galizia *et al*, 1997; Galizia and Menzel, 2000).

1.6. *Aims of the masters project*

In this project I intended to characterize, and define spatial and temporal characteristics of odour-evoked responses from one population of uPNs in the primary olfactory centre (AL) of the moth (*H. virescens*) brain using calcium imaging.

Principal aim: To determine overall responses in the AL evoked by biologically relevant odour compounds and their mixtures.

Specific aims:

- To successfully stain the glomeruli of the AL by retrograde labelling of PNs confined to the mALT.
- To observe and describe the overall spontaneous activity in the AL.
- To obtain time traces of glomerular responses to stimuli with corresponding AL maps.
- To explore how the MGC glomeruli respond to stimulation with single pheromone components versus a pheromone mixture.
- To describe the correlation of the responses of all glomeruli to all stimuli.

2. Materials and Methods

2.1. *Insects*

Throughout the duration of this study, the tobacco budworm moth *H. virescens* and the cotton bollworm moth *H. armigera* (Lepidoptera: Noctuidae: Heliothis) were used. *H. virescens* were reared in the laboratory: eggs were supplied by Bayer Crop Science AG (Mohnheim am Rhein, Germany) and larvae were reared on an artificial diet (Wu and Gong, 1997). *H. armigera* were acquired as pupae from China (Henan Jiyuan Baiyun Industry Co., Ltd. Pilot-Scale Base of Bio-pesticides, Institute of Zoology, Chinese Academy of Sciences). Immediately after arrival, *H. armigera* pupae were organized by gender into two separate Plexiglass containers with a pot of sucrose solution (100g/L of water) as a food source after hatching. Both *H. virescens* and *H. armigera* pupae were stored in temperature controlled heating cabinets (Binder KBWF, E5.2. + Refritherm 6E incubator, Struers) at 27°C with 70% air humidity and 23°C (respectively), and a 14 hour light, 10 hour dark photoperiod. Soon after hatching, both *H. virescens* and *H. armigera* were stored in new gender specific cylindrical Plexiglas containers with a pot of sucrose solution (100g/L of water), in a temperature controlled heating cabinet (Refritherm 6E incubator, Struers) at 23°C. Each cylinder permitted a certain number of moths. Five moths were distributed in the smaller cylinder, and eight in the larger cylinders (figure 2A, figure 2B respectively).

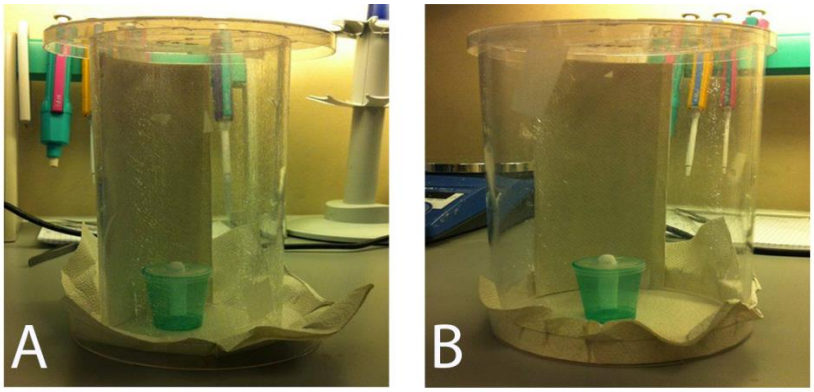

Figure 2: Examples showing the storage containers of the moths. **A.** Plexiglass container for five moths after hatching with pot of sucrose. **B.** Plexiglass container for eight moths after hatching with pot of sucrose.

2.2. *Moth preparation and staining process*

A distinct population of AL PNs, the uPNs innervating the calyces, were the target area for staining by inserting the fluorescent dye fura-dextran into the calyses of the MB. Thus, by applying fluorescent dye into the calyces, these neurons were successfully stained via retrograde labelling.

Moths were placed in a plastic stage, and secured at the neck using wax (Utility wax rods round, KERR corporation) to prevent transmission of movement from the legs, wings, and abdomen (figure 3A). A small amount of cotton wool was used to further immobilise the thorax and abdomen. The body was positioned so that the head, thorax, and abdomen were aligned. The head was tilted anteriorly and inferiorly by gently pulling on the proboscis to expose the area for dye injection and to obtain a better optical image of the area of investigation (left and right antennal lobes). The proboscis and mouth parts were sealed down using wax (figure 3A). Scales were removed using forceps and the exoskeleton was cleaned using wet tissue (figure 3B). Incisions were made using standard microdissecting equipment. Structures that can cause movement artifacts (muscles and trachea that connect the antennal lobe to muscle) were gently removed (figure 3C). The brain cavity was kept wet constantly by frequently rinsing it using saline solution (in mM: 150 NaCl, 3 CaCl2, 3 KCl, 25 sucrose, and 10 N-tris (hydroxymethyl)-methyl-2-amino-ethanesulfonic acid, pH 6.9) to prevent desiccation, remove cellular enzymes, and provide nutrition. Crystals of fura-dextran were coated on multiple glass electrodes, with two being injected into each of the left and right calyces (figure 3C). Moths were then left in a cool, dark insulated box with high humidity for the dye to take effect and reach target areas for a minimum of 4 hours. Incisions were made to remove the remaining exoskeleton, and the additional structures that can cause movement artifacts, as noted above, were gently removed (figure 3D). Antennae were fixed in the desired position using tungsten hooks (figure 3E). The preparations were covered with a coverslip and sealed using Kwik-Sil silicone elastomer (World Precision Instruments, inc. USA) (figure 3F).

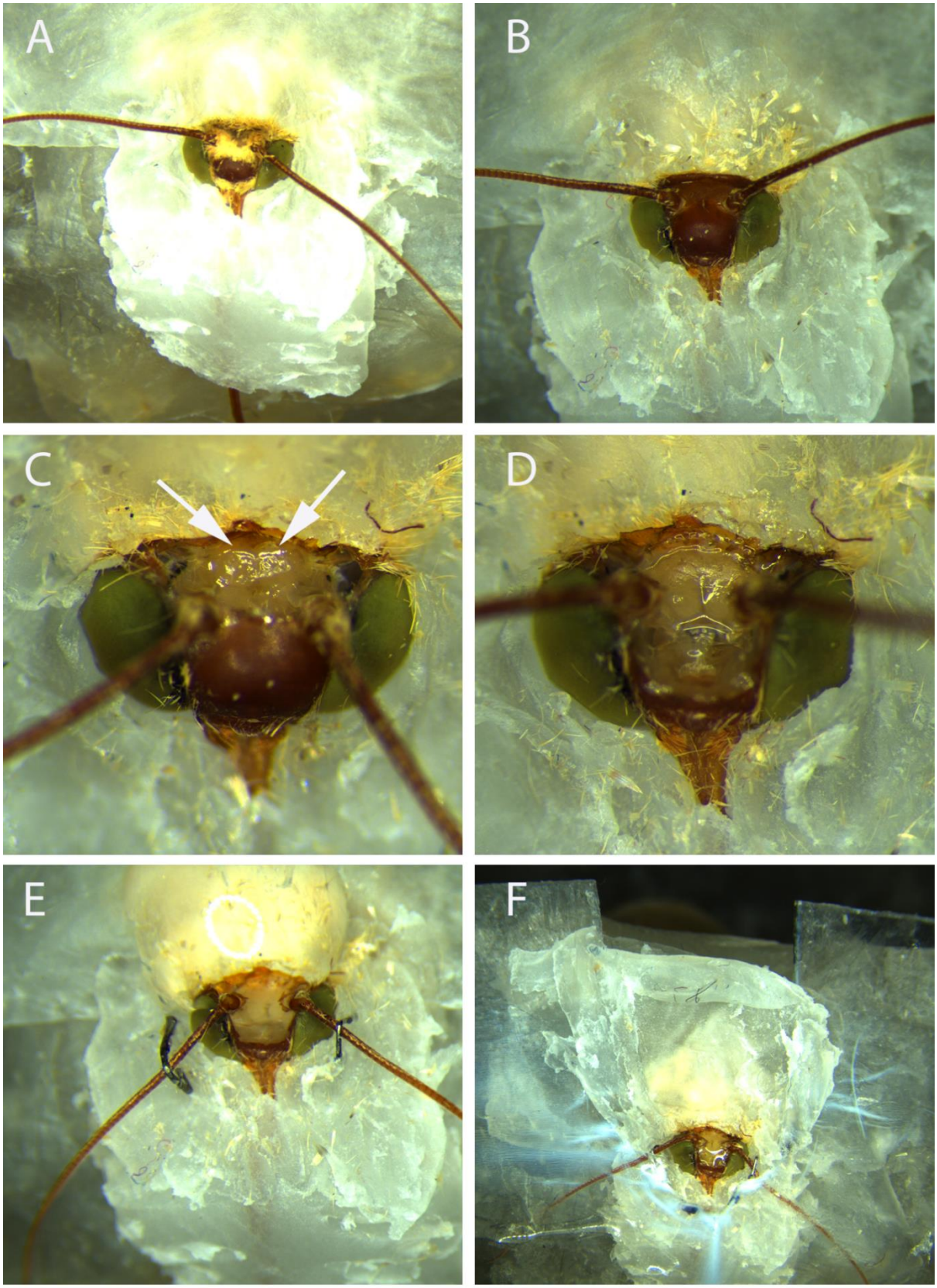

Figure 3: Series showing the different stages of the moth preparation. **A.** Moths placed in a plastic stage and immobilised. **B.** Scales removed and exoskeleton was cleaned. **C.** Removal of movement artifacts and injection of fura-dextran (indicated by arrows). **D.** Further removal of movement artifacts. **E.** Antennae fixation with tungsten hooks. **F.** Coverslip attached and sealed.

2.3. *Odour stimulation*

A constant airstream was applied to the antennae during non-stimulating and stimulating periods. A separate airstream containing the tested odour was used during stimulation. A two second odour burst was blown from the separate airstream into the constant airstream to initiate stimulation, with an inter stimulus interval (ISI) of approximately one minute. Each odour was delivered once and the entire stimulus sequence comprising all odours was conducted once only. Every odour was delivered manually, with intended triggering at the fortieth frame, and had a three second delay. Odour bursts lasted two seconds. All odours were mixed with hexane. 10µl of the individual odours was applied to individual pieces of filter paper, which were then evaporated and placed in clean glass cartridges. Different stimulus concentrations of the plant odours and pheromones were first tested for *H. armigera* before obtaining results to determine the concentrations inducing the optimal stimulus response. The optimal stimulus concentration was then used for both *H. armigera* and *H. virescens* whilst gathering data. A list of the plant odours, pheromones, and controls with their concentrations and amounts that were used are given in table 1 and table 2.

Table 1: Table showing the odour stimuli tested on *H. armigera*.

H. armigera				
Plant odour $10\mu l/10^{-2}$	**Pheromone** $10\mu l/10^{-4}$	**Pheromone mix (FM)** 50:50 $10\mu l/10^{-4}$	**Control** 10µl	**FM + Plant odour** $10\mu l/10^{-4}/10^{-4}$ respectively
Hexanyl Acetate	Z11-16:AL	Z11-16:AL + Z9-16:AL	Hexane	FM + Hexanyl acetate
Linalool	Z9-16:AL			FM + Linalool
Farnesene	Z9-14:AL			FM + Hexen-1-ol
Ocimene	Z11-16:OH			FM + Sunflower
Hexen-1-ol				
Sunflower headspace				

Table 2: Table showing the odour stimuli tested on *H. virescens*.

H. virescens				
Plant odour $10\mu l/10^{-2}$	**Pheromone** $10\mu l/10^{-4}$	**Pheromone mix (FM)** 50:50 $10\mu l/10^{-4}$	**Control** 10µl	**FM + Plant odour** $10\mu l/10^{-4}/10^{-2}$ respectively
Hexanyl Acetate	Z11-16:AL	Z11-16:AL + Z9-14:AL	Hexane	FM + Hexanyl acetate
Linalool	Z9-14:AL			FM + Linalool
Farnesene	Z11-16:AC			FM + Hexen-1-ol
Ocimene	Z11-16:OH			FM + Sunflower
Hexen-1-ol				
Sunflower headspace				

2.4. *Calcium measurements*

Moths were imaged under an upright Olympus BX5 1WI microscope with the 20x/0.50 water objective placed on top of the hole of the coverslip, in contact with the saline solution. The CCD camera (Evolve 512 EMCCD Camera, Photometrics) and imaging system was conducted using TILL photonics imaging system. Monochromatic excitation light alternated between 340 and 380 nm. Table 3 shows the protocol used for imaging. Pixel image size was 3.2 x 3.2µm, obtained by 4 x 4 binning on chip. For each stimulus 150 frames were taken at a frequency of 6.7Hz. All light sources were turned off during each stimulation process.

Table 3: Protocol used with TILL photonics imaging system for both *H. virescens* and *H. armigera*

Protocol	**Channel 1**	**Channel 2**
Wavelength (nm)	340	380
Exposure (ms)	40	30
Cycle (ms)	61	61
Loop count	100	100
Delay (ms)	28	
Total cycle (ms)	150	

2.5. *Data Processing*

2.5.1. *KNIME*

KNIME analytics platform version 2.12.2 (GmbH, Konstanz, Germany) (with ImageBee tool kit from Rein *et al*, 2013) was used. Important nodes were selected to import data from TILL photonics to KNIME for imaging videos to be processed (Image reader), with movement corrections of the data between submovies required (Stabiliser) due to a shift in the position of the AL between videos. Regions of interests (ROIs) were defined (Principal component analysis, (PCA)), and ROIs were recognised by fast PCA algorithm based on recognition of pixels that correlated with neighbouring pixels (Sampling PCA). Videos were Z transformed (Z score) and smoothened (Spatial filter) with Gaussian filter (kernel size 5) before the AL map was generated. The AL map was manually trimmed (rename components) to remove regions outside the limits of the AL. Movies were projected onto the generated AL map (Back project) to obtain glomerular time series for different glomeruli. These time series had raw $\frac{\Delta(F)}{F}$ calculated by subtracting the fluorescent level for each frame with each average fluorescent level. Raw $\frac{\Delta(F)}{F}$ was then imported into R-studio.

2.5.2. *R-studio*

ROI response filter was used to exclude all glomeruli that did not respond to stimuli more than $\pm$ 3SD from base line. Correlation was calculated for all stimuli pairs based on the time period where response occurred (frame 50-70) using a concatenated vector over all glomeruli. False colour plot was used to plot correlations. The quantified response strength between two variables was analysed: the relative maximum amplitude of the signal relative to onset (baseline), and the integral of calcium traces within the response window relative to base line (using trapezoid function). For time traces, values are given as

$$\frac{\Delta(\mathrm{F})}{\mathrm{F}} = \frac{F_{i-F_0}}{F_0} \times 100$$

F_i indicates the fluorescence intensity in frame i, F_0 indicates the fluorescence intensity at baseline. Quantile-Quantile plot of data and histograms was run to check the normality of the variables distribution. T-test was conducted to look at the relative maximum amplitude and integral to compare response strength across stimuli.

2.6. *Ethics*

When conducting research on animals there are laws concerning their welfare in the form of ethics, which incorporate vertebrates. These laws however do not extend to all species of invertebrates, Lepidoptera included. As such, there are no restrictions regarding their use in research, nor is ethical approved required. Regardless of the lack of ethics available to Lepidoptera, all moths were treated with the utmost care. This care included daily inspection of their containers, the replenishment of their food source, regular cleaning of the paper at the bottom and on the sides of their containers for hygiene purposes, and limiting the number of moths per container to avoid space related stress. During experimentation, as much care and consideration was given to the moths that the procedures allowed.

3. Results

Out of the 70 male animal preparations completed, the results of this investigation were obtained from nine successful preparations in total, five of which were from *H. armigera,* and four from *H. virescens*. Both species of moth possess different compounds that are produced by the females for communication, which occur within and across the different species. Although the MGCs of these moth species have slight differences, the general organisation of the olfactory pathways share strong similarities (Berg *et al,* 2014). The investigations conducted and the results presented in this paper include: spontaneous activity and the presence of successfully stained glomeruli, the production of time traces with corresponding AL maps, the effects of ternary mixtures on the whole AL, the effect of using single pheromone components against a pheromone mixture in the MGC, and the correlation of the responses of all glomeruli to all stimuli.

3.1. *Criteria for successfully stained preparations*

When determining which of the animal preparations were suitable for experimentation, certain criteria had to be met. This criteria includes successfully stained glomeruli (figure 4), and the observation of spontaneous activity (data not shown). These criterion were observed in the raw data. Different types of spontaneous activity were observed in the raw data (data not shown). When observing the AL as a video clip it was possible to detect spontaneous activity in the AL as individual glomeruli continuously flickering in different light intensities. The spontaneous activity of the glomeruli indicates that the uPNs were successfully stained.

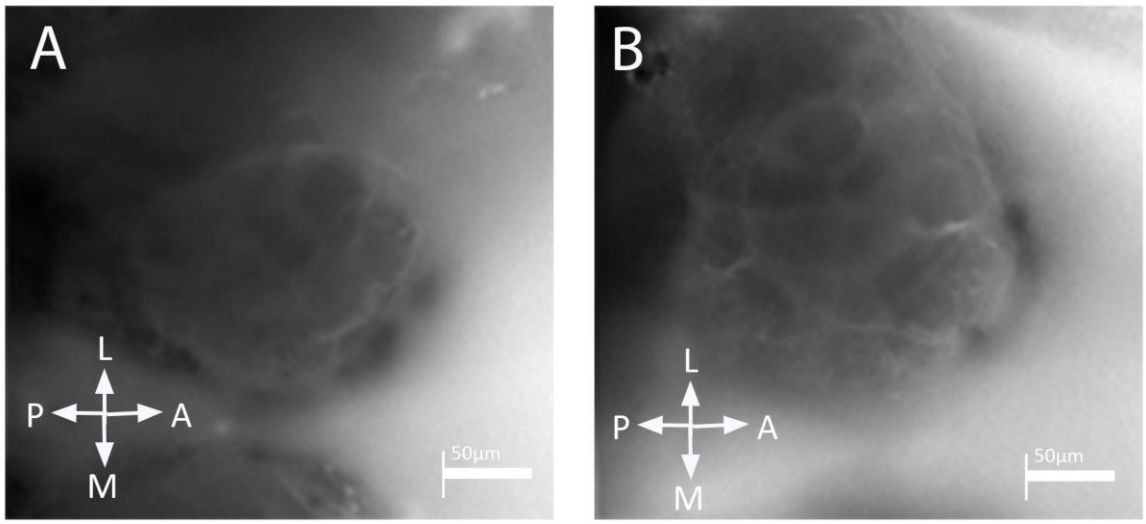

Figure 4: Animals with successfully met criteria for further experimentation (stained glomeruli in the antennal lobes (AL) of both moth species) **A**. Raw ratio data from the left AL of *H. armigera* showing successfully stained glomeruli. Orientation indicated (A = anterior, M = medial, P = posterior, L = lateral). Scale bar represents size of one glomerulus. **B**. Raw data from the left AL of *H. virescens* showing successfully stained glomeruli. Orientation indicated (A = anterior, M = medial, P = posterior, L = lateral). Scale bar represents the approximate diameter of one ordinary glomerulus, i.e. 50 µm.

3.2. *Time traces and glomerular maps*

Having completed processing of the raw data, time traces of stimuli response and AL maps were generated to further the analysis of the effects of using different plant odours and pheromones as stimuli in the AL. All single stimuli components had induced calcium responses in different glomerular combinations in the AL. A change in calcium responses to single stimuli components were able to be reproduced between individual animals tested on (data not shown).

Glomerular responses to single plant odorants

All plant odours tested elicited glomerular responses. Figure 5 to figure 11 shows examples of time traces generated from the same single animal of *H. virescens*, including activation patterns of the strongest responding glomeruli to plant odour stimuli. It was possible to determine which glomeruli responded to a particular stimulus by using the numbered AL map to look for the corresponding region of interest (ROI) number allocated to the time traces. This could be observed in all animals tested on. It was also possible to visualise the responses on the accompanying peak excitation map.

Generally, linalool elicited the strongest response in all ROIs (figure 5). The ROI's that showed the strongest consistent responses in figures 5 through 11 were ROI 2, ROI 3, ROI 6,

ROI 7, ROI 14, and ROI 20. Of these, the strongest responding ROI to all plant odour stimuli was ROI 2. The remaining consistently responding ROIs are clustered around this strongest responding ROI. Stimulation with farnesene (figure 6) elicited glomerular responses that resembled the responses from hexen-1-ol glomeruli (figure 7). Hexanyl acetate glomerular responses (figure 8) are akin to the glomerular responses to ocimene (figure 9), and linalool glomerular responses (figure 5) are comparable to sunflower glomerular responses (figure 10). Control (figure 11) caused relatively lower glomerular responses; although ROI 2 had a response which was comparable to hexanyl acetate (figure 8) and ocimene (figure 9). Figure 12 shows all the glomerular responses to all the plant odour stimuli pooled into the time traces where comparisons can be made.

MGC responses to female-produced substances

Female-produced compounds were also tested. Figure 13 to figure 17 shows examples of time traces and activation patterns induced by this kind of stimuli, generated from the same single animal of *H. virescens* as referred to above. The ROIs shown in figure 13 to figure 17 are the strongest responding glomeruli. Some of these ROIs may correspond to the MGC units. The numbered AL map was used again to determine which glomeruli responded to a particular stimulus by looking for the corresponding ROI number allocated to the time traces. Again, it was possible to visualise the responses on the accompanying peak excitation map.

The single female-produced component that evoked the strongest responses in all ROIs was Z11-16:AL, which is the major pheromone constituent of *H. virescens* (figure 13). The ROIs that showed the strongest consistent responses and may be included in the MGC, were ROI 4, ROI 16, and ROI 24 (see figures 13 through 17). Of these, ROI 16 often elicited the strongest response to the female-produced stimuli tested. The remaining consistently strong responding ROIs are positioned on either side of this strongest responding ROI. The responses to Z9-14:AL, the second pheromone component of *H. virescens*, were the smallest (figure 14). Generally, the responses elicited by the pheromone mixture were the strongest among all responses induced by the female-produced stimuli (figure 15). As shown in figure 16, one of the interspecific signals, Z11-16:AC, elicited a strong response in ROI 4, a weak response in ROI 16, and no response in ROI 24. The interspecific signal, Z11-16:OH, also evoked a response in all ROIs (figure 17), although smaller than those induced by the major pheromone component. Figure 18 shows all the glomerular responses of all the female-produced stimuli pooled into the time traces where comparisons can be made. It is important to note that although these stimuli produced the responses in what may be the MGC, they

also produced responses in what is clearly the part of the AL that responds to plant odour stimuli; these ROIs are not commented on in this paragraph. ROI 2, for example, is obviously included in the responding glomeruli, as demonstrated on the accompanying peak excitation map in figures 13 through 17.

By looking at the AL map and the corresponding ROI in each animal it was also possible to establish that stimuli were activating the correct area of the AL, i.e. plant odours were activating the area of the AL responsible for processing plant odour stimuli, not the MGC which is responsible for processing pheromone.

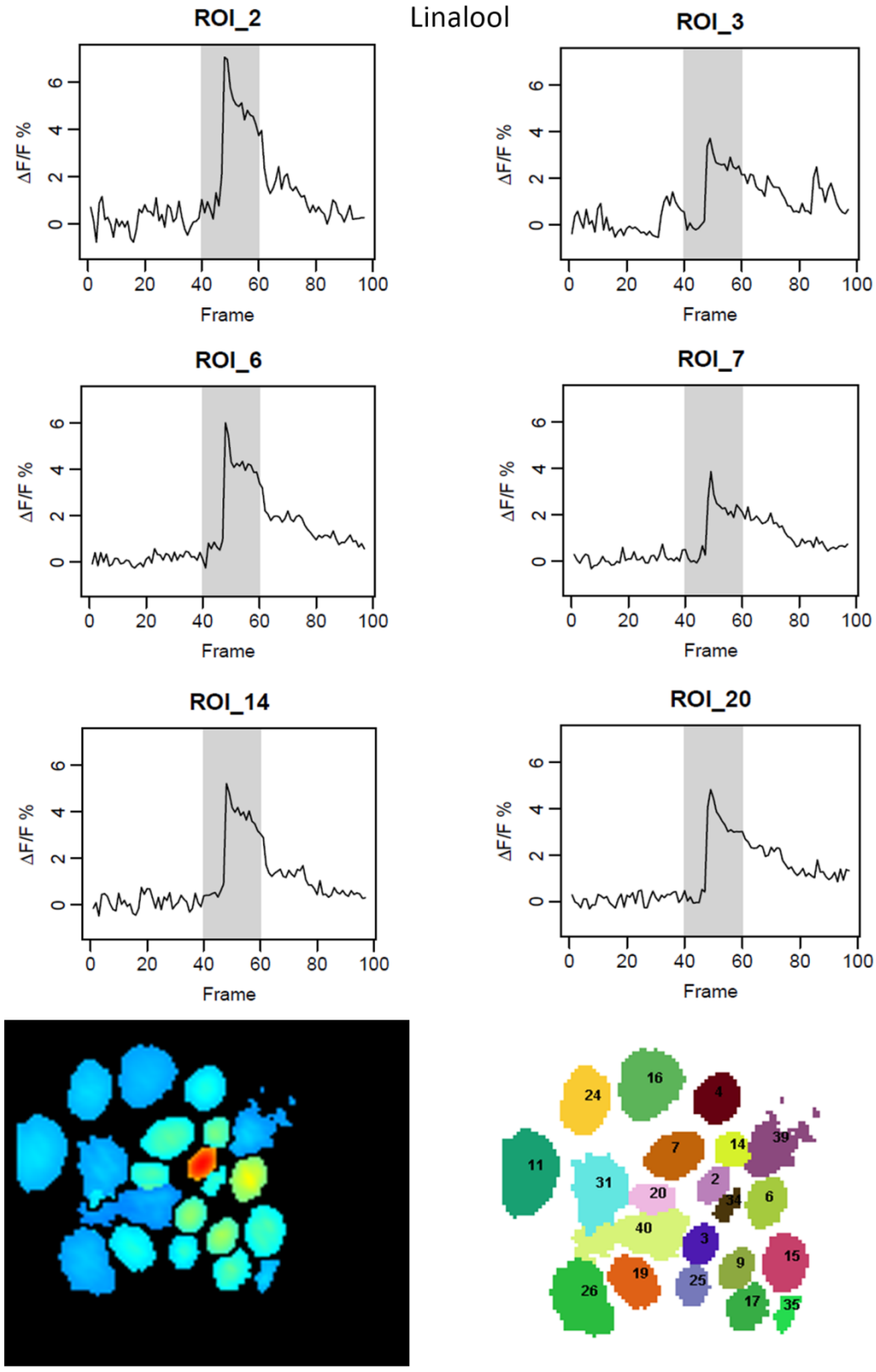

Figure 5: Time traces showing the best responding glomeruli (region of interest (ROI)) in *H. virescens* to linalool. Location of ROI's can be found on the corresponding numbered antennal lobe (AL) map. Responses can be visualised on the accompanying peak excitation map (Dark blue = no response, lighter blue = some response, orange = strong response, red = very strong response). For time traces, stimulus onset begins at intended stimulus window (frame 40), response measured as ΔF/F%.

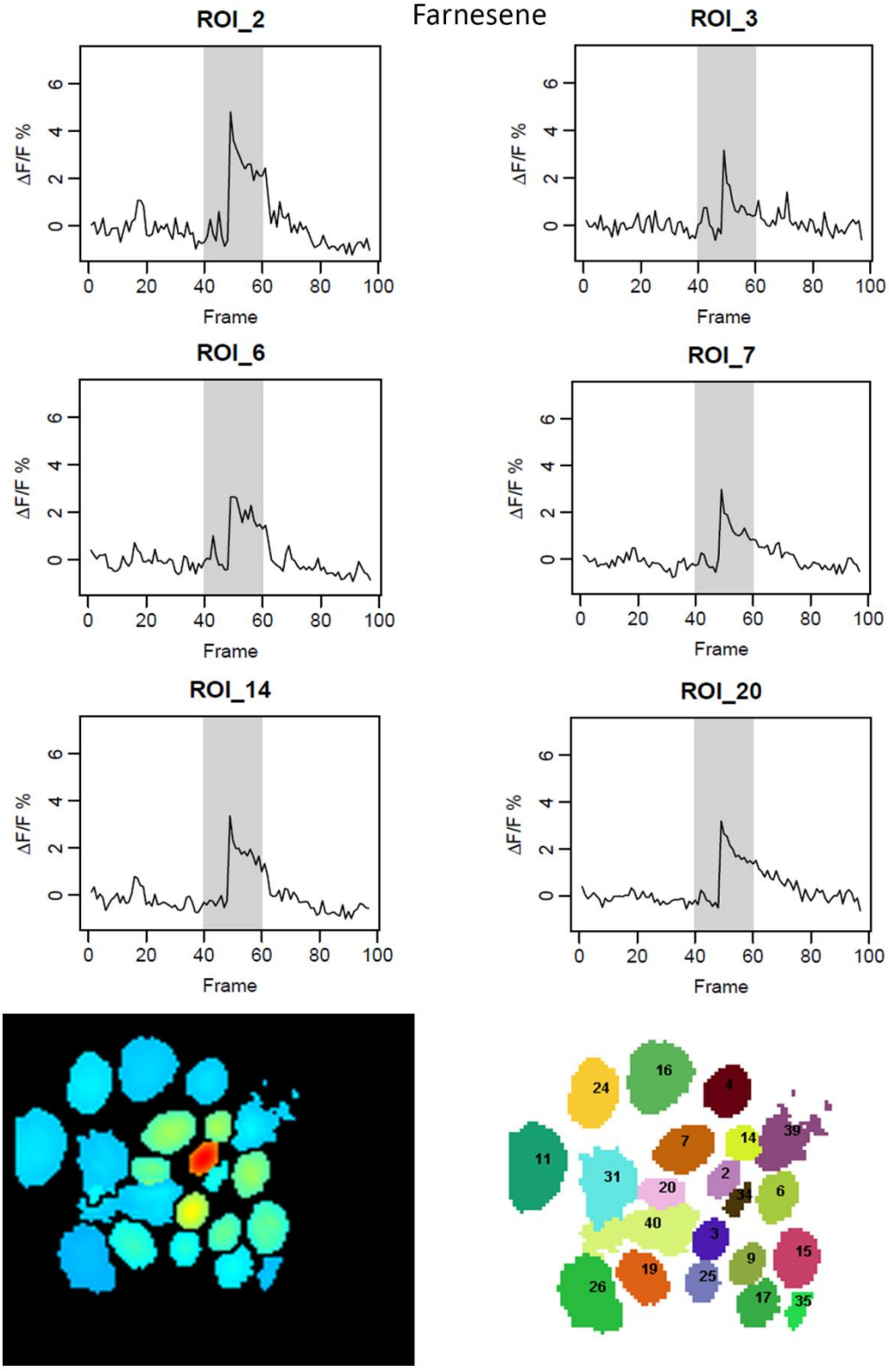

Figure 6: Time traces showing the best responding glomeruli (region of interest (ROI)) in *H. virescens* to farnesene. Location of ROI's can be found on the corresponding numbered antennal lobe (AL) map. Responses can be visualised on the accompanying peak excitation map (Dark blue = no response, lighter blue = some response, orange = strong response, red = very strong response). For time traces, stimulus onset begins at intended stimulus window (frame 40), response measured as ΔF/F%.

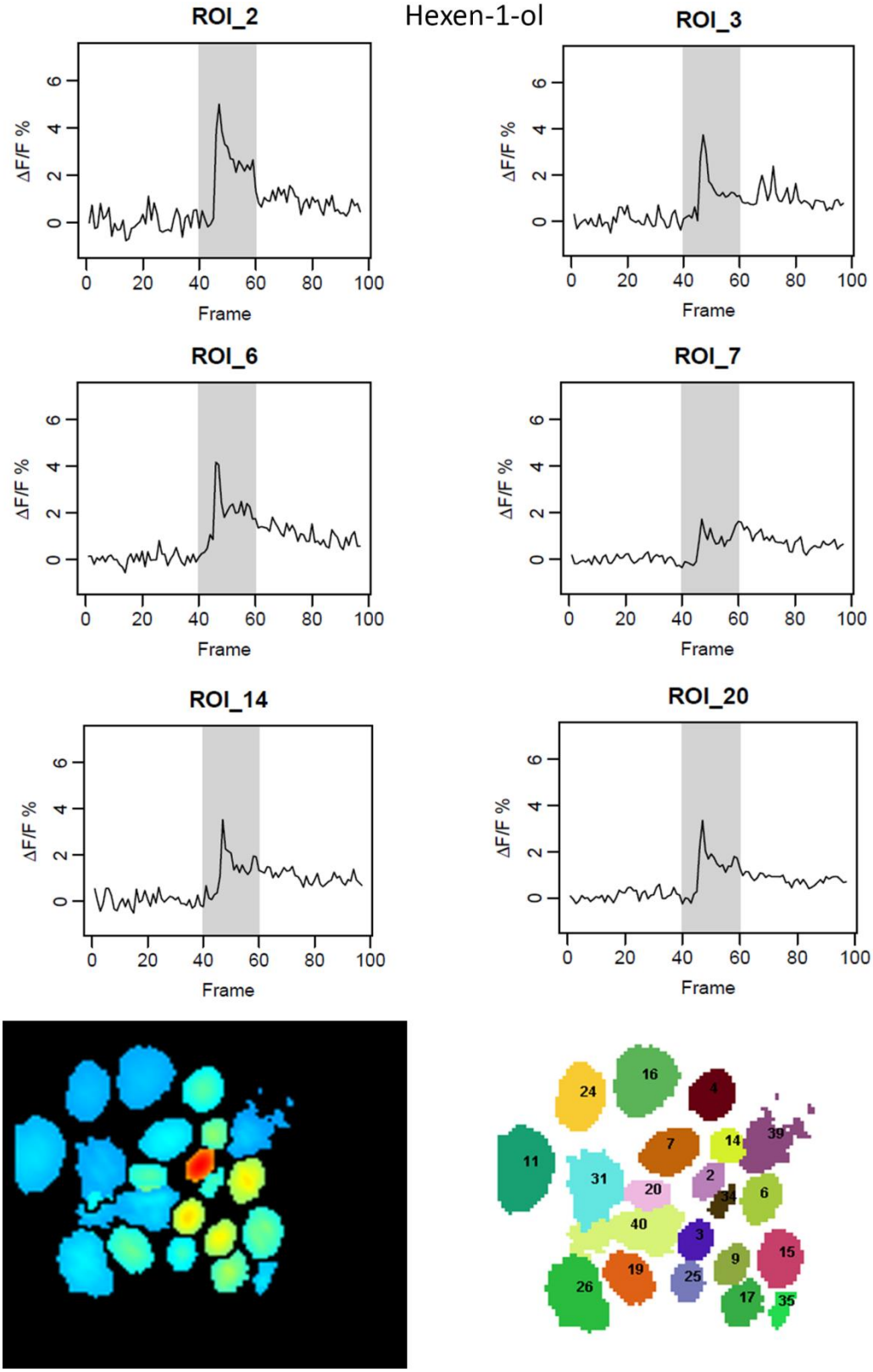

Figure 7: Time traces showing the best responding glomeruli (region of interest (ROI)) in *H. virescens* to hexen-1-ol. Location of ROI's can be found on the corresponding numbered antennal lobe (AL) map. Responses can be visualised on the accompanying peak excitation map (Dark blue = no response, lighter blue = some response, orange = strong response, red = very strong response). For time traces, stimulus onset begins at intended stimulus window (frame 40), response measured as ΔF/F%.

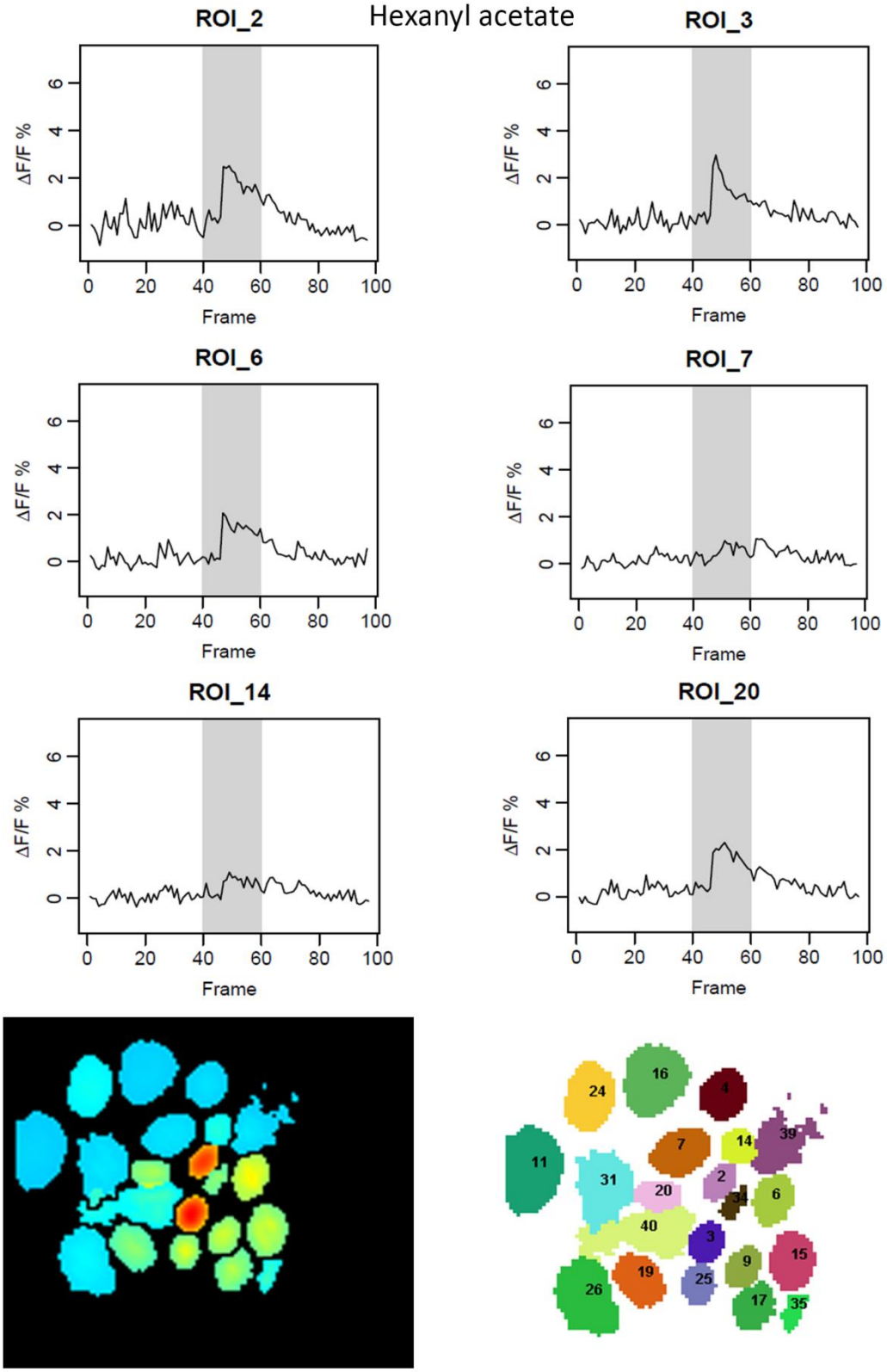

Figure 8: Time traces showing the best responding glomeruli (region of interest (ROI)) in *H. virescens* to hexanyl acetate. Location of ROI's can be found on the corresponding numbered antennal lobe (AL) map. Responses can be visualised on the accompanying peak excitation map (Dark blue = no response, lighter blue = some response, orange = strong response, red = very strong response). For time traces, stimulus onset begins at intended stimulus window (frame 40), response measured as ΔF/F%.

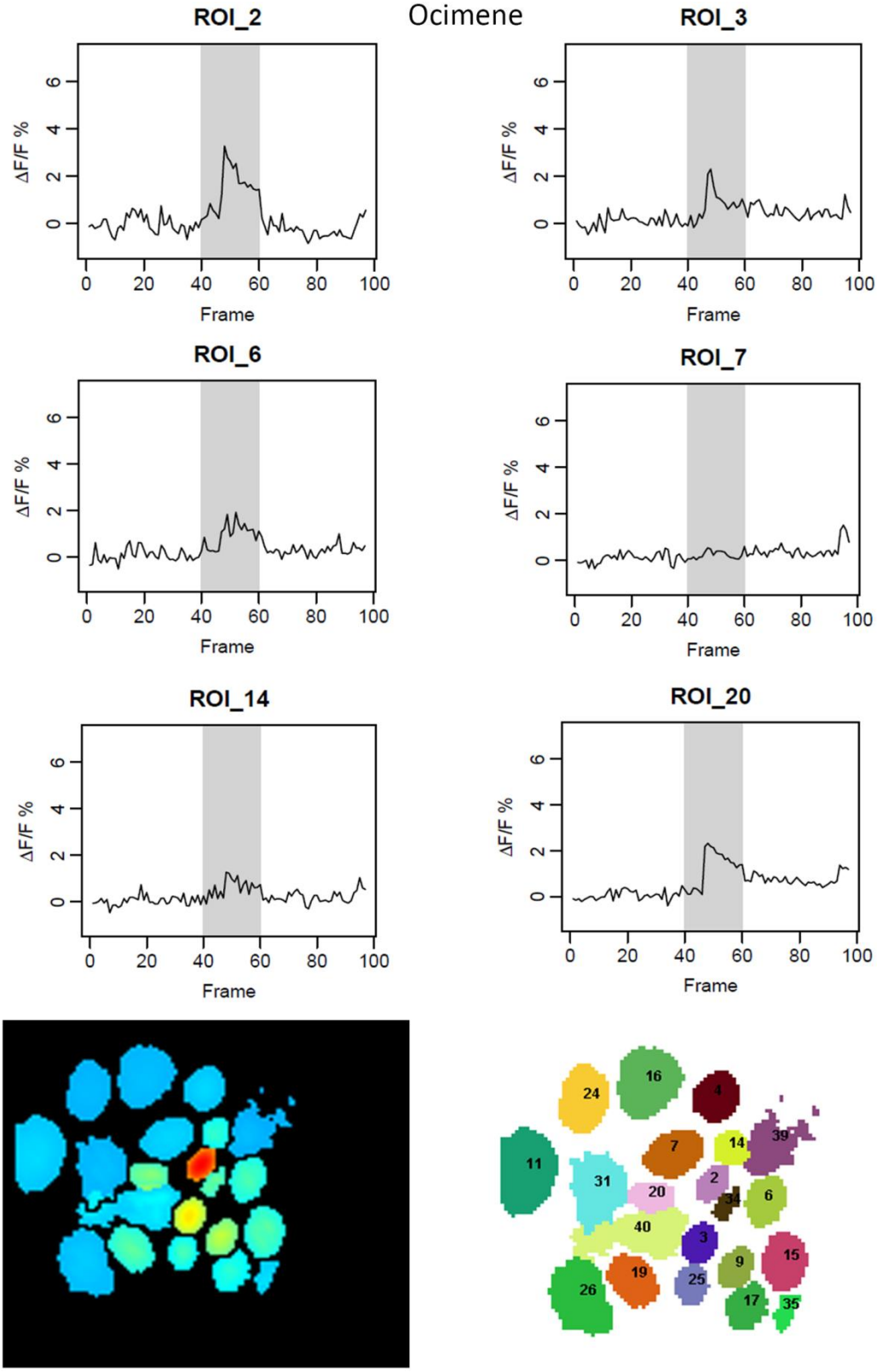

Figure 9: Time traces showing the best responding glomeruli (region of interest (ROI)) in *H. virescens* to ocimene. Location of ROI's can be found on the corresponding numbered antennal lobe (AL) map. Responses can be visualised on the accompanying peak excitation map (Dark blue = no response, lighter blue = some response, orange = strong response, red = very strong response). For time traces, stimulus onset begins at intended stimulus window (frame 40), response measured as ΔF/F%.

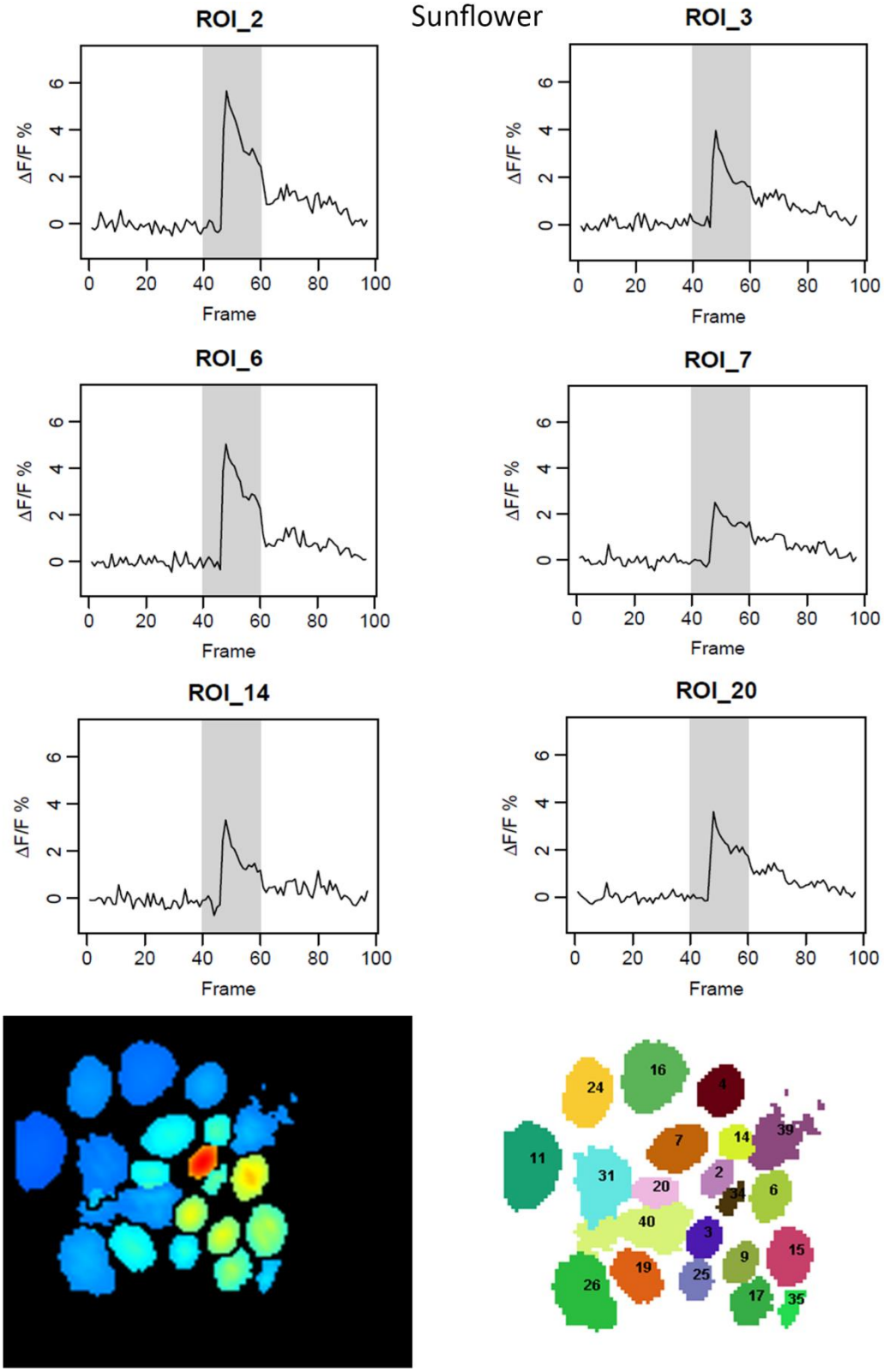

Figure 10: Time traces showing the best responding glomeruli (region of interest (ROI)) in *H. virescens* to sunflower. Location of ROI's can be found on the corresponding numbered antennal lobe (AL) map. Responses can be visualised on the accompanying peak excitation map (Dark blue = no response, lighter blue = some response, orange = strong response, red = very strong response). For time traces, stimulus onset begins at intended stimulus window (frame 40), response measured as ΔF/F%.

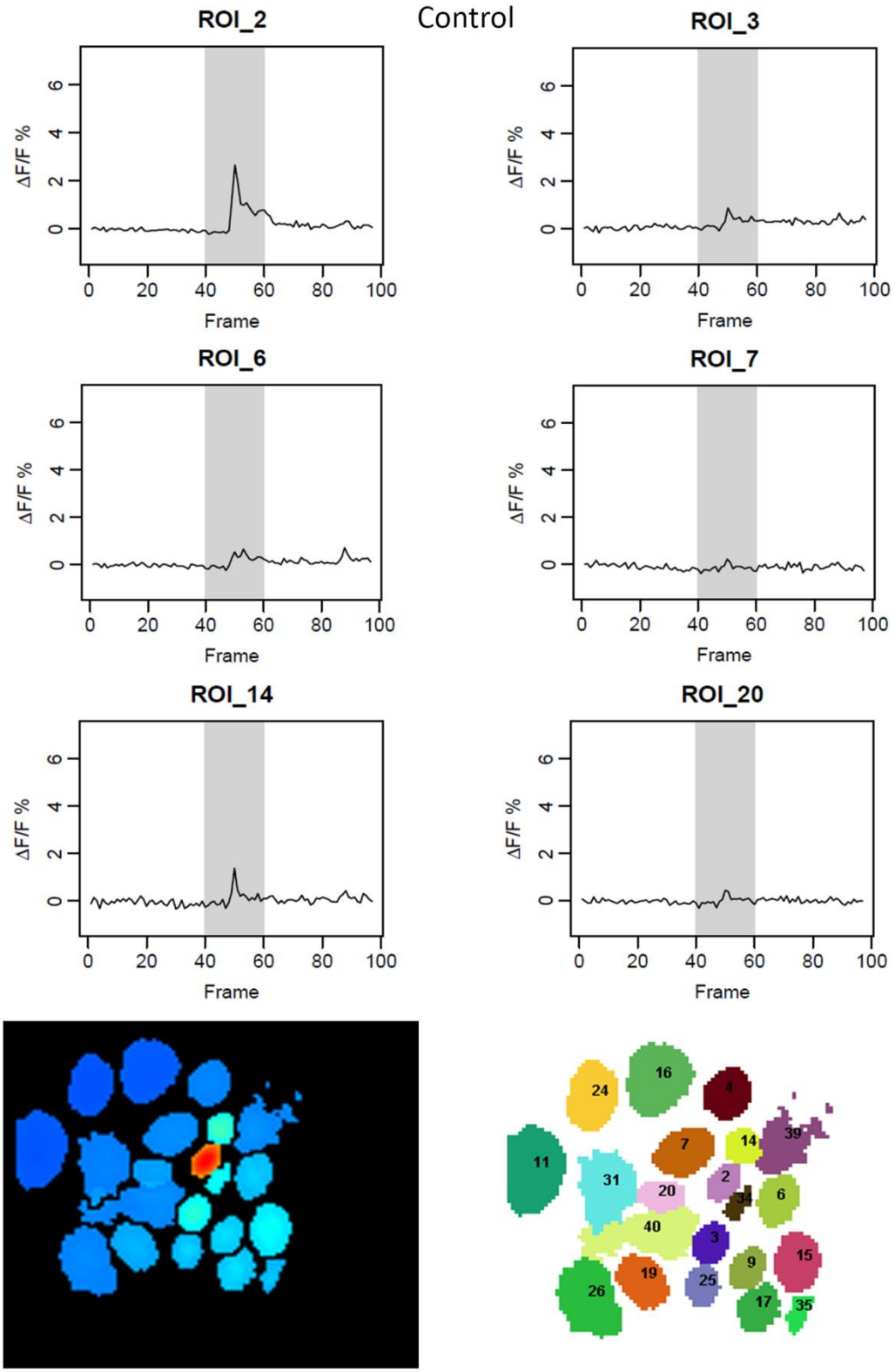

Figure 11: Time traces and glomerular maps showing the best responding glomeruli in *H. virescens* to control. The responses are visualised on the accompanying peak excitation map (Dark blue = no response, lighter blue = some response, red = very strong response). Location of the responding glomeruli of interest (region of interest (ROI)) can be found on the corresponding numbered antennal lobe (AL) map. For time traces, stimulus onset begins at intended stimulus window (frame 40), response measured as ΔF/F%.

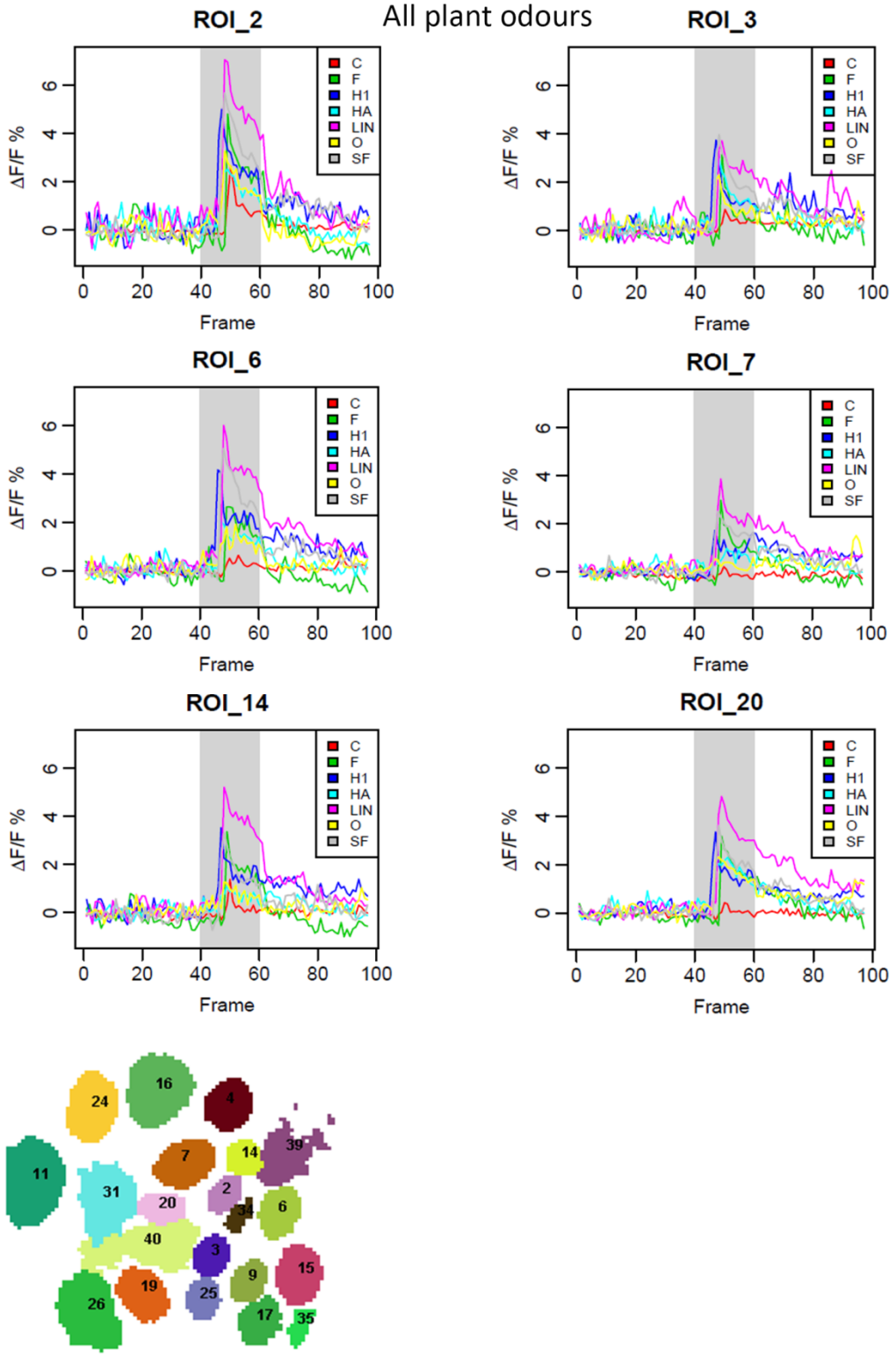

Figure 12: Time traces showing the best responding glomeruli (region of interest (ROI)) in *H. virescens* to all plant odours (C=control, F=farnesene, H1=hexen-1-ol, HA=hexanyl acetate, LIN=linalool, O=ocimene, SF=sunflower). Location of ROI's can be found on the corresponding numbered antennal lobe (AL) map. For time traces, stimulus onset begins at intended stimulus window (frame 40), response measured as ΔF/F%.

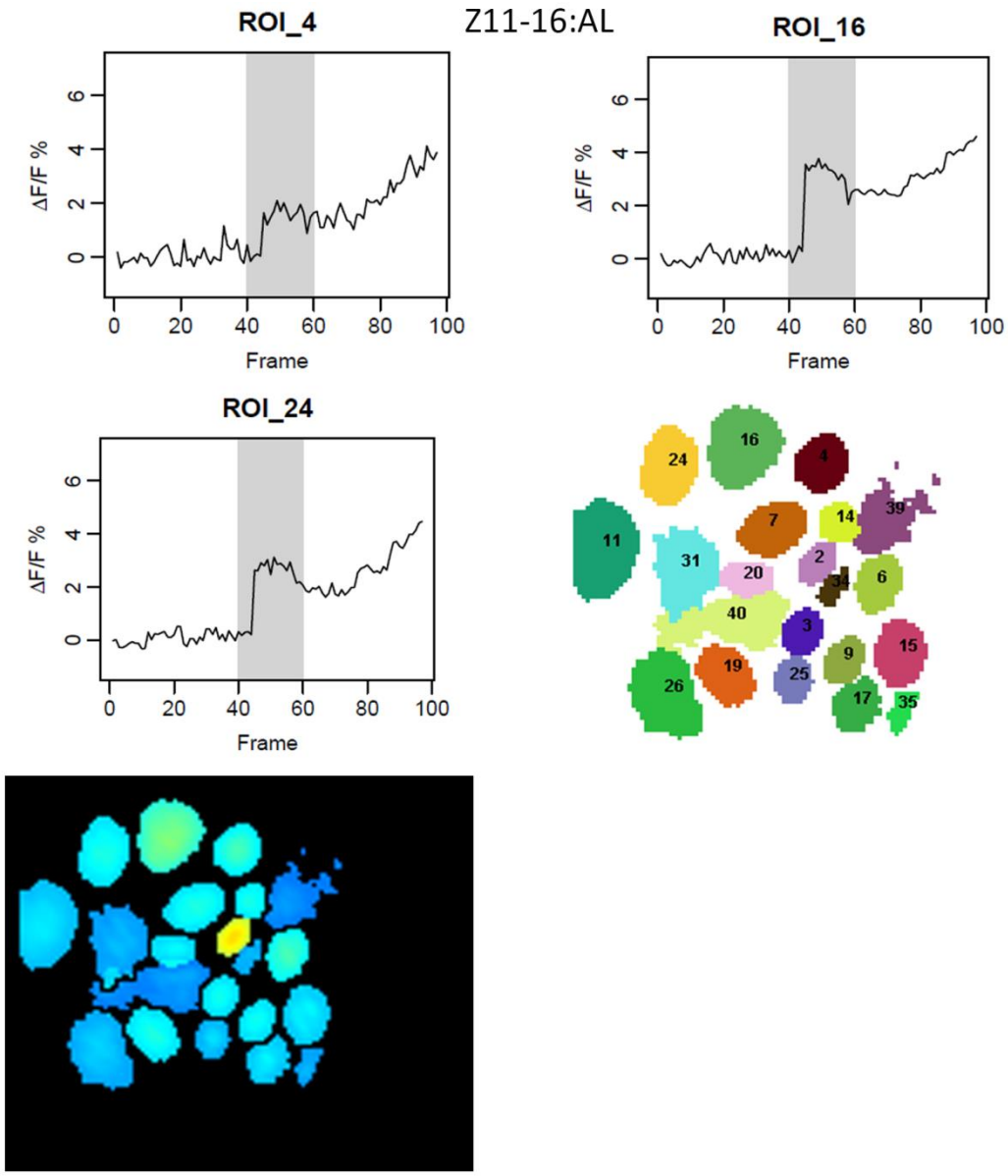

Figure 13: Time traces showing glomeruli that may resemble the macroglomerular complex (MGC) in *H. virescens* responding to Z11-16:AL. Location of region of interests (ROIs) can be found on the corresponding numbered antennal lobe (AL) map. Responses can be visualised on the accompanying peak excitation map (Dark blue = no response, lighter blue = some response, orange = strong response, red = very strong response). For time traces, stimulus onset begins at intended stimulus window. Stimulus onset begins at intended stimulus window (frame 40), response measured as ΔF/F%.

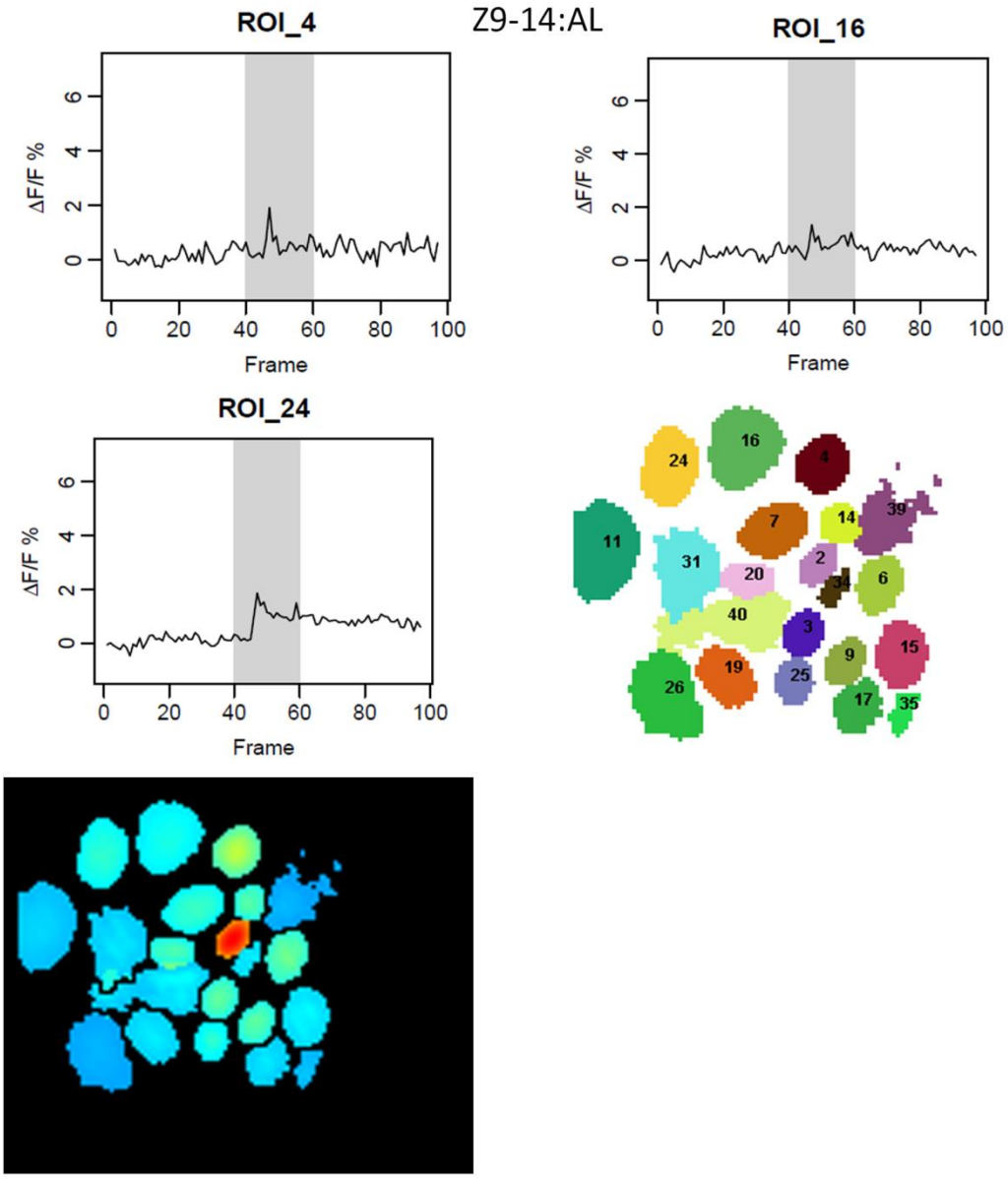

Figure 14: Time traces showing glomeruli that may resemble the macroglomerular complex (MGC) in *H. virescens* responding to Z9-14:AL. Location of region of interests (ROIs) can be found on the corresponding numbered antennal lobe (AL) map. Responses can be visualised on the accompanying peak excitation map (Dark blue = no response, lighter blue = some response, orange = strong response, red = very strong response). For time traces, stimulus onset begins at intended stimulus window. Stimulus onset begins at intended stimulus window (frame 40), response measured as ΔF/F%.

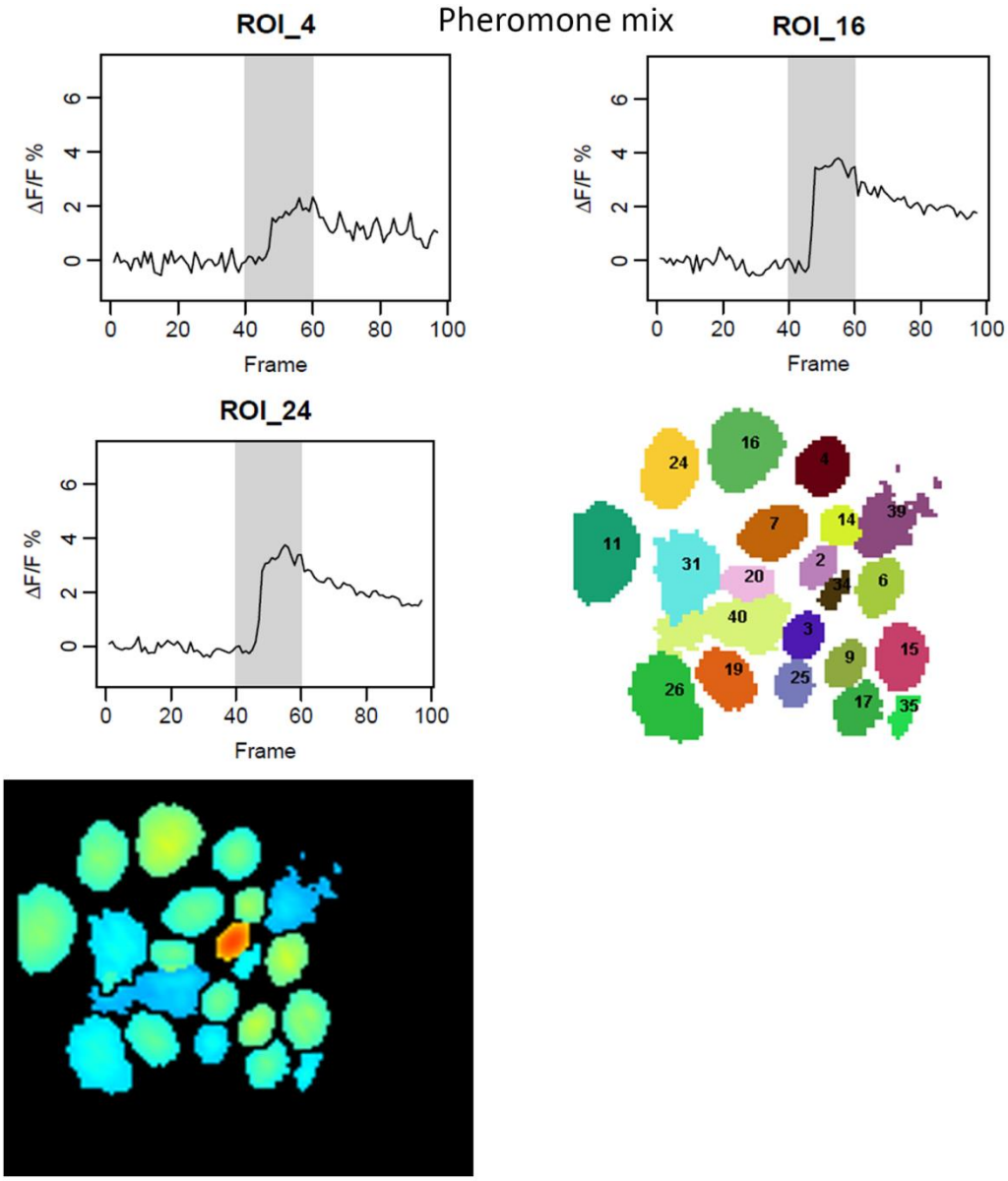

Figure 15: Time traces showing glomeruli that may resemble the macroglomerular complex (MGC) in *H. virescens* responding to the pheromone mixture (Z11-16:AL + Z9-14:AL). Location of region of interests (ROIs) can be found on the corresponding numbered antennal lobe (AL) map. Responses can be visualised on the accompanying peak excitation map (Dark blue = no response, lighter blue = some response, orange = strong response, red = very strong response). For time traces, stimulus onset begins at intended stimulus window. Stimulus onset begins at intended stimulus window (frame 40), response measured as ΔF/F%.

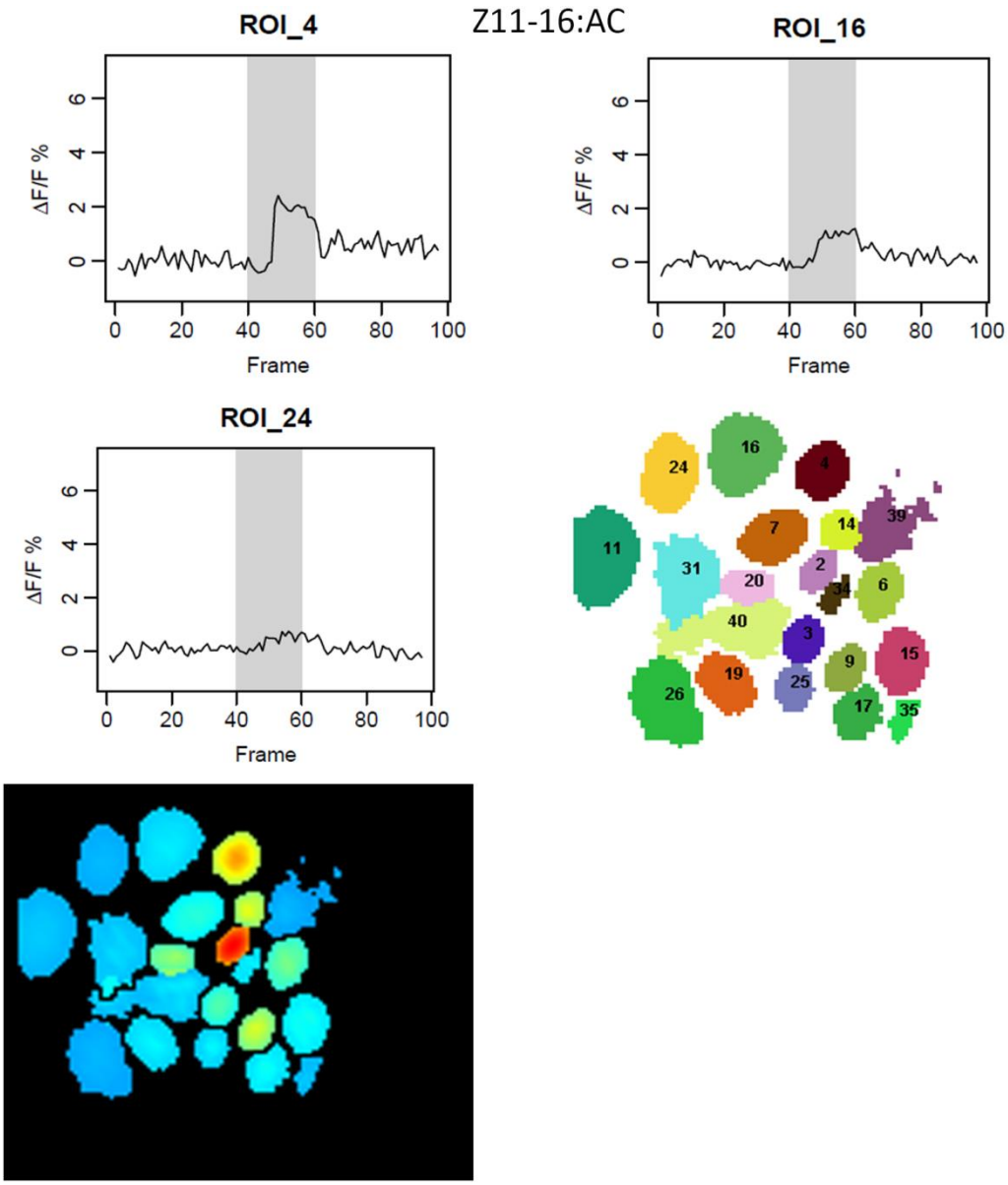

Figure 16: Time traces showing glomeruli that may resemble the macroglomerular complex (MGC) in *H. virescens* responding to Z11-16:AC. Location of region of interests (ROIs) can be found on the corresponding numbered antennal lobe (AL) map. Responses can be visualised on the accompanying peak excitation map (Dark blue = no response, lighter blue = some response, orange = strong response, red = very strong response). For time traces, stimulus onset begins at intended stimulus window. Stimulus onset begins at intended stimulus window (frame 40), response measured as ΔF/F%.

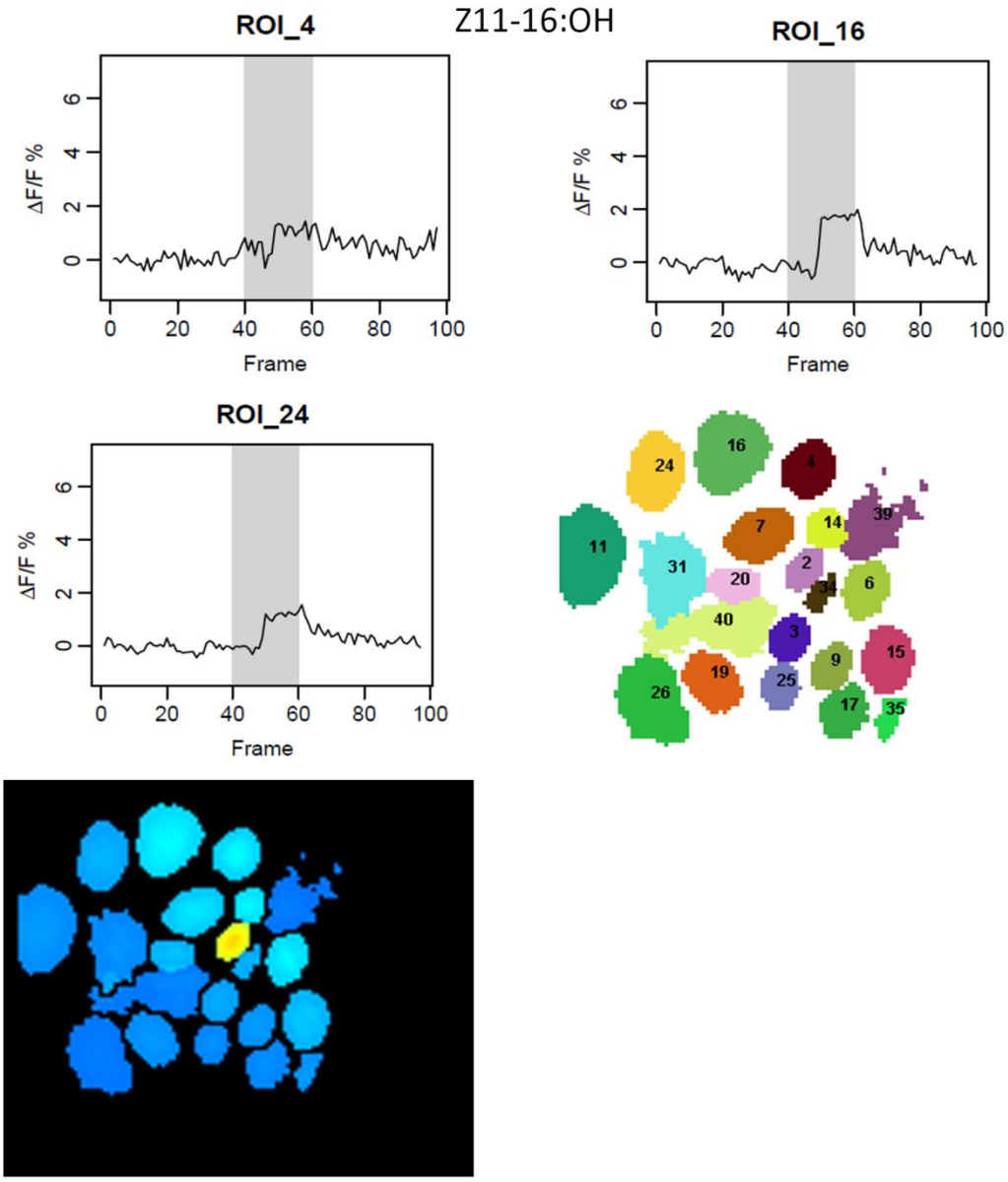

Figure 17: Time traces showing glomeruli that may resemble the macroglomerular complex (MGC) in *H. virescens* responding to Z11-16:OH. Location of region of interests (ROIs) can be found on the corresponding numbered antennal lobe (AL) map. Responses can be visualised on the accompanying peak excitation map (Dark blue = no response, lighter blue = some response, orange = strong response, red = very strong response). For time traces, stimulus onset begins at intended stimulus window. Stimulus onset begins at intended stimulus window (frame 40), response measured as ΔF/F%.

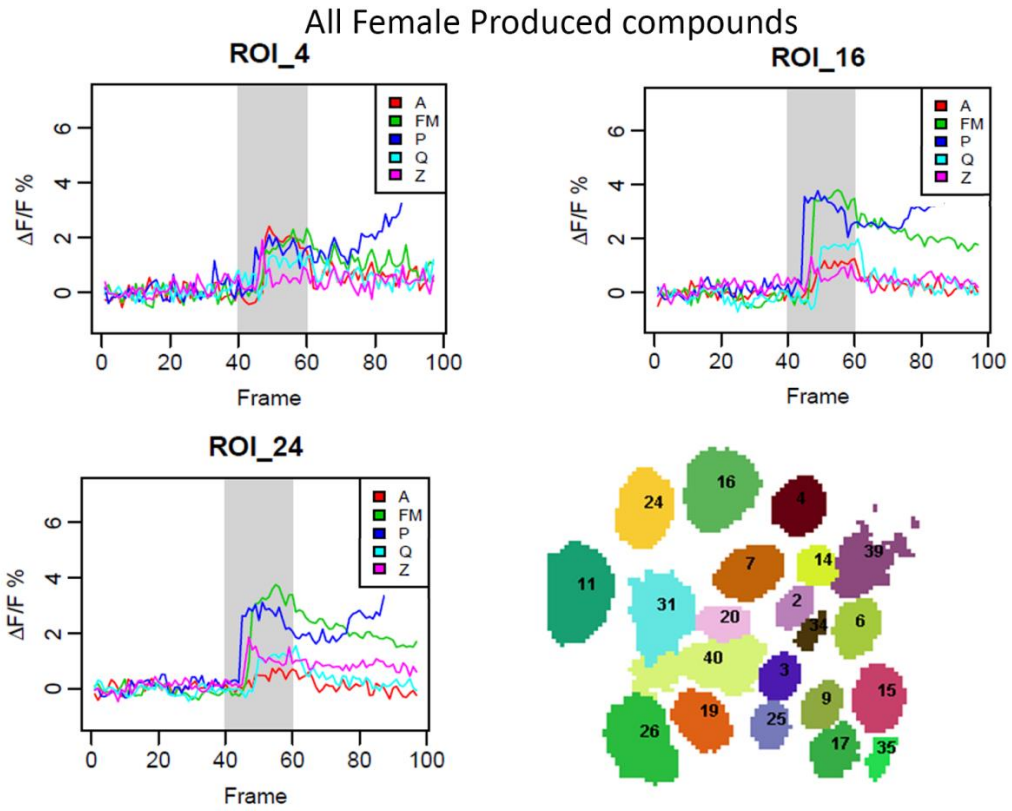

Figure 18: Time traces showing glomeruli that may resemble the macroglomerular complex (MGC) in *H. virescens* responding to all pheromones (A=Z11-16:AC, FM=pheromone mixture (Z11-16:AL + Z9-14:AL), P=Z11-16:AL, Q=Z11-16:OH, and Z=Z9-14:AL) . Location of region of interests (ROIs) can be found on the corresponding numbered antennal lobe (AL) map. For time traces, stimulus onset begins at intended stimulus window. Stimulus onset begins at intended stimulus window (frame 40), response measured as ΔF/F%.

3.3. *Effects of ternary mixtures on the whole AL*

In addition to testing plant odours and pheromones separately, the effect of a blend consisting of the two pheromone components and one plant odorant (ternary mixture) was investigated. In the examples presented here, the principal pheromones for *H. vir*escens, Z11-16:AL and Z9-14:AL, were tested together with one of the following plant odour substances: sunflower, linalool, hexanyl acetate, and hexen-1-ol. The responses elicited by these four odour mixtures were recorded from 269 glomeruli in a total of 14 ALs (of *H. virsescens*). The data presented shows that there was an observable difference between the responses of single stimuli and ternary stimuli.

Effect of pheromones on plant odour evoked responses

Generally, the data demonstrate that the presence of the natural pheromone suppresses plant odour-evoked responses in the AL. Figure 19A shows the relative maximum amplitude of glomerular responses to stimuli measured as $max\frac{\Delta(\mathrm{F})}{\mathrm{F}}$. The bar graph highlights how the presence of pheromone affects the representation of plant odours in the whole AL, and identifies that there was an overall suppressive effect (a lower glomerular response to plant/pheromone mixtures than to the single plant odour stimuli). All the four plant odours elicited weaker responses when they were combined with the pheromone mixture than when tested alone (paired t-test, $P = 3.1 \times 10^{-4}$) (Figure 19A).

The suppressive effect of the pheromones was particularly obvious for the responses including sunflower (SF) and pheromone mix (FM) (paired t-test, $P = 2.5 \times 10^{-11}$), and Hexen-1-ol (H1) and FM (paired t-test, $P = 0.043$), which corresponded to a 26% and 10% lower response to the mixtures than to the plant odour alone, respectively (Figure 19A) (see figure 20B for time trace showing an example of suppression, where 'FM' + 'SF' in green results in weaker response than 'SF' in blue alone). There were however, a few cases of synergy (a greater glomerular response to the pheromone/plant odour mixtures than to the single plant odour stimuli). This applies to hexanyl acetate (HA) and FM, for example (paired t-test, $P = 5.6 \times 10^{-4}$) (figure 19A), which corresponds to 19% larger response of the mixture than of the plant odour alone (see figure 20A for time trace showing an example of synergy, where 'FM' + 'HA' in green results in stronger response than 'HA' in blue alone). Also, hypoadditivity (equal glomerular responses to mixtures and the single stimuli) was observed for linalool (LIN) and FM (paired t-test, $P = 0.79$), which corresponds to 1% larger response of the mixtures (Figure 19A). Unpaired t-test was also completed for the control

(hexane) against all plant odours combined with the pheromone mixture and the plant odours alone ($P = 1.02 \times 10^{-11}$), which corresponded to a 28% lower response than plant odour combined with the pheromone mixtures and plant odours alone (data not shown).

Following the calculation of the relative maximum amplitude, the integral was also looked at. Figure A1 in the appendix shows the integral of the glomerular response window to stimuli measured as $\int \frac{\Delta(F)}{F}$. The bar graph highlights how the presence of pheromone affects the representation of plant odours in the whole AL, and in contrast to figure 19A, identifies that there was no significant overall suppressive effect of all the plant odours combined with the pheromone mixture than the plant odours alone after paired t-test was completed ($P = 0.33$) (figure A1, appendix). Unpaired t-test was also completed for the control (hexane) against all plant odours combined with the pheromone mixture and the plant odours alone ($P = 1.2 \times 10^{-10}$), which corresponded to a 35% lower response than plant odour combined with the pheromone mixtures and plant odours alone (data not shown).

Although there was no significant overall suppressive effect shown, for each pair of ternary mixtures, similar effects were seen in comparison to figure 19A: A suppressive effect in the mixtures for 'SF' and 'FM' (paired t-test, $P = 5.6 \times 10^{-5}$), and 'H1' and 'FM' (paired t-test, $P = 0.03$), which corresponded to a 23% and 18% lower response of the mixtures than plant odour alone, respectively (figure A1, appendix), as well as a few cases of synergy for 'HA' and 'FM' (paired t-test, $P = 1.6 \times 10^{-6}$), and hypoadditivity in 'LIN' and 'FM' (paired t-test, $P = 0.13$), which corresponded to 51% and 9.9% larger response of the mixtures than plant odour alone, respectively (figure A1, appendix).

Effect of plant odours on pheromone-evoked responses

Except for one case, including sunflower (SF), the data shows that the presence of plant odours has no effect on the pheromone-response. Figure 19B shows the relative maximum amplitude of responses to stimuli measured as $\max \frac{\Delta(F)}{F}$. The bar graph highlights how the presence of plant odours affects the representation of pheromone signals in the whole AL. Following an unpaired t-test for three of the combinations of plant odours with 'FM' (figure 19B), it was shown that approximately the same number of glomeruli were activated across the whole AL for 'H1' with 'FM', 'HA' with 'FM', and 'LIN' with 'FM' than 'FM' alone ($P = 0.86$, $P = 0.97$, and $P = 0.06$ respectively). After an unpaired t-test had been conducted for the combination of 'SF' with 'FM', there was significantly more glomeruli activated across the whole AL than 'FM' alone ($P = 3.3 \times 10^{-5}$). An unpaired t-test for the control (C)

against ‘FM’ showed that significantly fewer glomeruli were activated for ‘C’ than ‘FM’ (P = 0.001) (figure 19B).

Figure A2 in the appendix shows the integral of the glomerular response window to stimuli measured as $\int \frac{\Delta(F)}{F}$. The bar graph highlights how the presence of plant odours affects the representation of pheromone signals in the whole AL. Again, similar effects were seen in comparison to figure 19B: Unpaired t-test for the combination of ‘SF’ with ‘FM’, showed there was significantly more glomeruli activated across the whole AL than ‘FM’ alone (P = 5.6×10^{-5}) (figure A2, appendix), unpaired t-test for ‘HA’ with ‘FM’, and ‘LIN’ with ‘FM’ (figure A2, appendix), showed that approximately the same number of glomeruli were activated across the whole AL than ‘FM’ alone (P = 0.92, and P = 0.12 respectively), but unpaired t-test showed that significantly less glomeruli were activated across the whole AL for ‘H1’ with ‘FM’ (P = 0.04) . An unpaired t-test for ‘C’ against ‘FM’ showed that significantly fewer glomeruli were activated for ‘C’ than ‘FM’ (P = 7.01×10^{-5}) (figure A2, appendix).

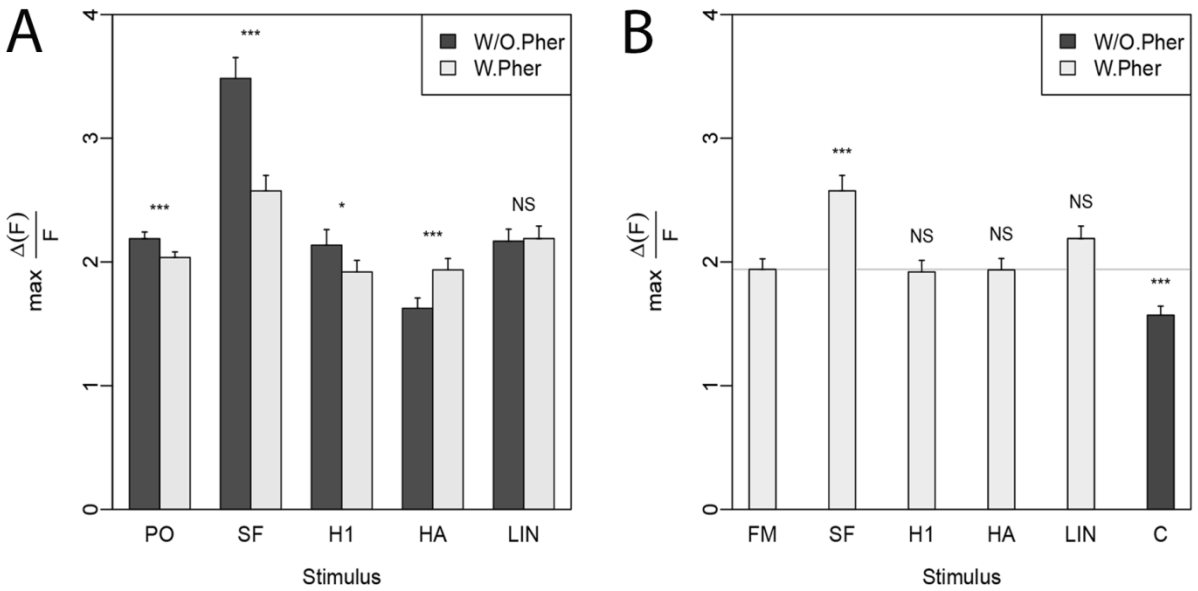

Figure 19: Bar graph representing the relative maximum amplitude of the effects of pheromones on plant odour evoked responses and the effects of plant odours on pheromone-evoked responses**. A.** Bar graph showing the pooled data of the relative maximum response of glomeruli (measured as $max\frac{\Delta(F)}{F}$) to different stimuli (PO = All plant odours, FM = pheromone mix, SF = Sunflower, H1 = Hexen-1-ol, HA = Hexanyl acetate, LIN = Linalool) combined with 'FM' (W.Pher) vs. Without 'FM' (W/O. Pher), to determine how the presence of pheromone affects the representation of plant odours in the whole antennal lobe (AL). Standard error means are shown with stars indicting *P*-value (* = 0.05, ** = 0.01, *** = 0.001, NS = >0.05). **B**. Bar graph showing the pooled data of the relative maximum response of glomeruli (measured as $max\frac{\Delta(F)}{F}$) to different stimuli ('FM', 'SF', 'H1', 'HA', and 'LIN') combined with 'FM' Vs. 'FM' alone, to determine how adding plant odours affects the representation of pheromone signals in the whole antennal lobe (AL). Control (C) was measured against 'FM'. Standard error means are shown with stars indicting *P*-value (* = 0.05, ** = 0.01, *** = 0.001, NS = >0.05).

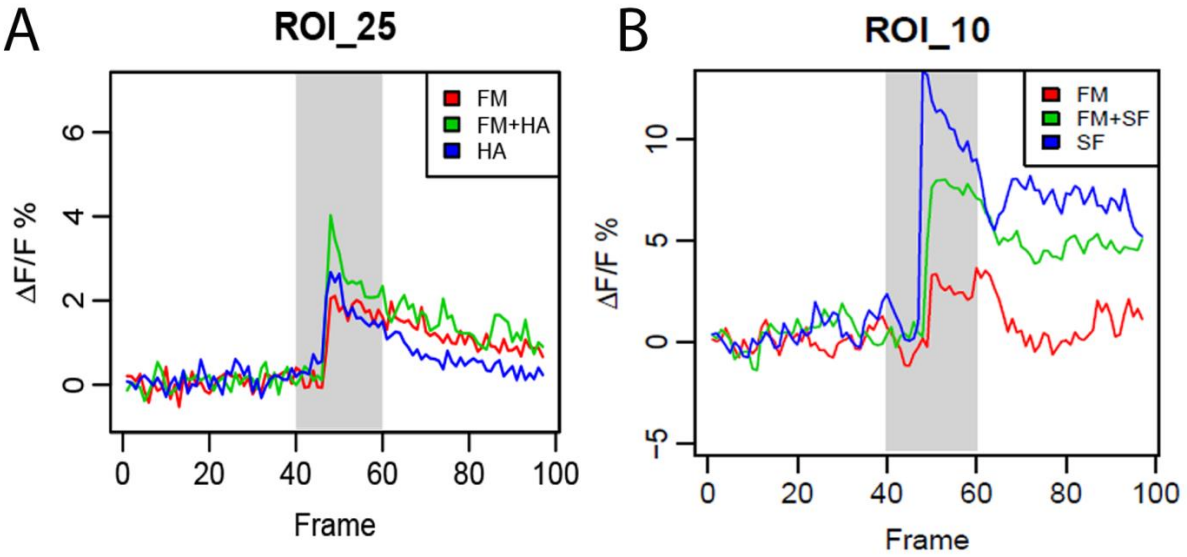

Figure 20: Time traces representing examples of synergy and suppression. **A.** Time trace showing an example of a synergy effect on plant odour glomeruli ('FM' + 'HA' in green results in stronger response than 'HA' in blue alone) from pooled data. Stimulus onset begins at frame 40, response measured as ΔF/F%. **B.** Time trace showing an example of a suppressive effect on plant odour glomeruli ('FM' + 'SF' in green results in weaker response than 'SF' in blue alone) from pooled data. Stimulus onset begins at frame 40, response measured as ΔF/F%.

3.4. *Effects of pheromone mixture and single pheromone components in the MGC*

To determine the effects of using the pheromone mixture (comprised of the primary and secondary pheromone components), compared to the primary and secondary pheromone components alone, as well as the interspecific signals, the integral of the glomerular response window to the pheromones of *H. viriscens* and *H. armigera* measured as $\int \frac{\Delta(F)}{F}$, were plotted into a bar graph (figure 21). The bar graphs show the MGC responses to the different pheromone stimuli and compare the strength of response elicited by single pheromone components to that induced by the pheromone blend, plus the response strength of control. Paired t-test was performed on all pheromones and pheromone mixtures against control.

Figure 21A represents the pooled data of both moth species and shows the MGC responses to control (C), the primary pheromone component, Z11-16:AL (P), and pheromone mixture (FM) (see below for species specific components). T-test results showed that the response of 'P' from the pooled data was significantly greater than 'C' (P = 0.008, which corresponds to 96% larger response). Also, the response to 'FM' was significantly greater than that to 'C' (P = 0.002, which corresponds to 154% larger response) (figure 21A). It was also shown in figure 21A that the response to 'FM' was greater than the response to 'P'.

Figure 21B represents the responses in the MGC of *H. armigera* to 'C', the primary pheromone component Z11-16:AL (P), the secondary pheromone component Z9-16:AL (S), FM (Z11-16:AL + Z9-16:AL), and the interspecific signals, Z9-14:AL (Z) and Z11-16:OH (Q). The results of the t-tests in figure 21B showed that none of the components used had a significant response. The components that had a greater response than 'C' were 'P' (P = 0.21), 'Q' (P = 0.59), with the greatest being 'FM' (P = 0.06), which corresponded to an increase in 28%, 21%, and 64% respectively (figure 21B). The components with a lower response than 'C' were 'S' (P = 0.09) and 'Z' (P = 0.15), which corresponded to 51% and 33% lower response respectively (figure 21B).

Figure 21C represents the responses in the MGC of *H. viriscens* to 'C', the primary pheromone component Z11-16:AL (P), the secondary pheromone component Z9-14:AL (Z), FM (Z11-16:AL + Z9-14:AL), and the antagonist pheromone components Z11-16:AC (A) and Z11-16:OH (Q). After having conducted t-tests of the pheromone components, the results show that 'P', 'FM', 'A', and 'Q' had a significantly stronger response than 'C' (P = 0.005, P = 0.004, P = 0.01, P = 0.002 respectively), with 'FM' having the strongest response (figure 21C). Although 'Z' had a stronger response than 'C', it was not significant (P = 0.16).

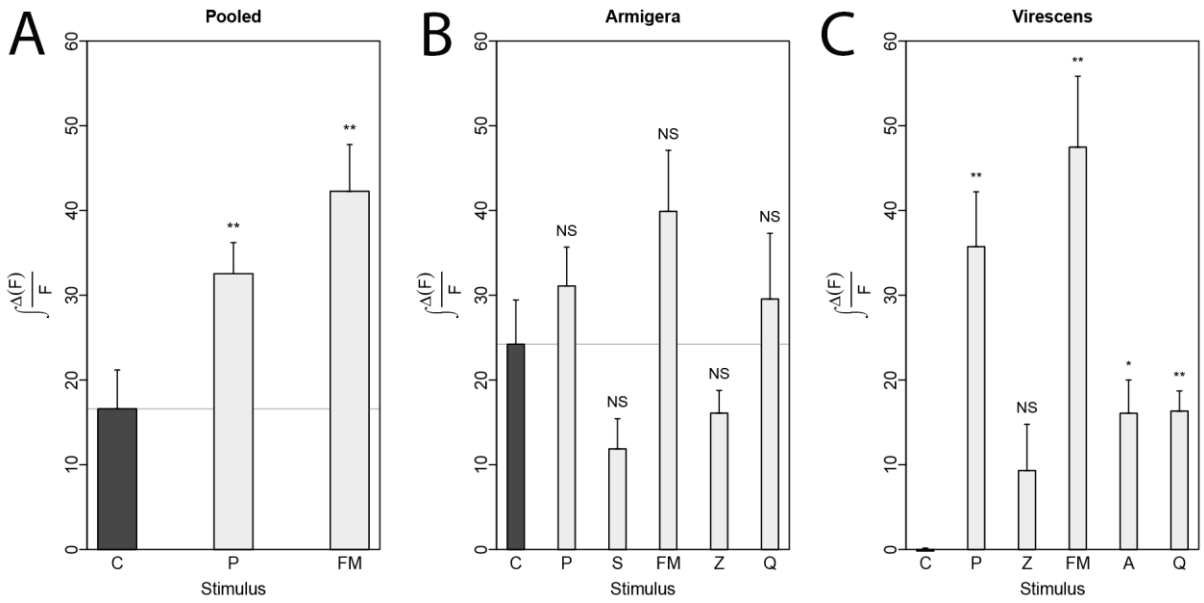

Figure 21: Bar graphs representing the integral glomerular responses in the MGC to female produced compounds. **A.** Pooled data of *H. viriscens* and *H. armigera* presented as a Bar graph showing the glomerular response in the macroglomerular complex (MGC), measured as $\int \frac{\Delta(F)}{F}$, to pheromone stimuli using a pheromone mixture, composed of the primary and secondary pheromone components, compared to the primary pheromone component alone of both species (C = control, P = primary component Z11-16:AL, FM = pheromone mixture). Standard error means are shown with stars indicting *P*-value (* = 0.05, ** = 0.01, *** = 0.001, NS = >0.05). **B**. Bar graph showing the glomerular response in the MGC of *H. armigera* to species specific pheromone stimuli, measured as $\int \frac{\Delta(F)}{F}$, using a pheromone mixture composed of the primary and secondary pheromone components (FM = Z11-16:AL + Z9-16:AL), compared to the primary component Z11-16:AL (P) and secondary pheromone component Z9-16:AL (S) alone, as well as to the antagonistic components Z9-14:AL (Z) and Z11-16:OH (Q), and control (C). Standard error means are shown with stars indicting *P*-value (* = 0.05, ** = 0.01, *** = 0.001, NS = >0.05). **C**. Bar graph showing the glomerular response in the MGC of *H. viriscens* to species specific pheromone stimuli, measured as $\int \frac{\Delta(F)}{F}$, using a pheromone mixture composed of the primary and secondary pheromone components (FM = Z11-16:AL + Z9-14:AL), compared to the primary component Z11-16:AL (P) and secondary pheromone component Z9-14:AL (Z) alone, as well as to the antagonistic components Z11-16:AC (A) and Z11-16:OH (Q), and control (C). Standard error means are shown with stars indicting *P*-value (* = 0.05, ** = 0.01, *** = 0.001, NS = >0.05).

3.5. *Correlation of all glomerular responses to all stimuli*

Every response, from every recordable glomeruli to all plant odour stimuli and ternary mixtures, from every recordable AL used in this investigation was correlated and plotted into a correlation matrix graph (figure 22A). Each pixel in the graph represents the average response of all glomeruli that responded to that particular stimuli. All plant odour stimuli possessed a weak correlation with each other, (r) ranging from 0.1 - 0.4, with the exception of linalool (LIN) and sunflower (SF) which had a moderate correlation with each other (r = 0.5). 'LIN' appeared to be the only plant odour that weakly correlated with all other plant odours, whereas the remaining plant odours weakly correlated with one, two, or three other plant odours (figure 22A). All plant odours also weakly correlated with the control (r = 0.2 – 0.5). Figure 22A also shows there was a weak negative correlation between the primary pheromone component (P) and all ternary mixtures, as well as with all plant odours save hexen-1-ol (H1) which was strongly correlated (r = 0.7). 'P' also had a moderate correlation with the pheromone mixture (FM) (r = 0.4).

A subset of responses of the 269 glomeruli to stimuli reported in figure 4 was also correlated and plotted into a correlation graph (figure 22B). Each pixel in the graph represents the average response of all glomeruli that responded to that particular stimuli. It is important to note that the colour ranges differ between figure 22A and figure 22B, due to each graph having been calculated on base of range of correlation from two data sets. As it was shown in figure 22A, there was again a weak correlation amongst the plant odours, (r) ranging from 0.1 – 0.4, with the exception of 'SF' and 'LIN' which had a moderate correlation seen, (r) ranging between 0.5 – 0.6 (figure 22B). There was a moderate to strong correlation observed between all the ternary stimuli (pheromone mixtures combined with the plant odour), than between the plant odours alone, with 'FM' + 'HA' and 'FM' + 'H1', and 'FM' + 'SF' and 'FM' + 'HA' having the strongest correlation (r = 0.7) (figure 22B). There were also weak correlations between the ternary stimuli and the respective plant odour alone, as well as an extremely weak positive or extremely weak negative correlation between 'FM' and the plant odours alone, and a weak correlation between 'FM' and the ternary mixtures, with the exception of 'FM' and 'FM' + 'HA' which was moderately correlated (r = 0.7) (figure 22B).

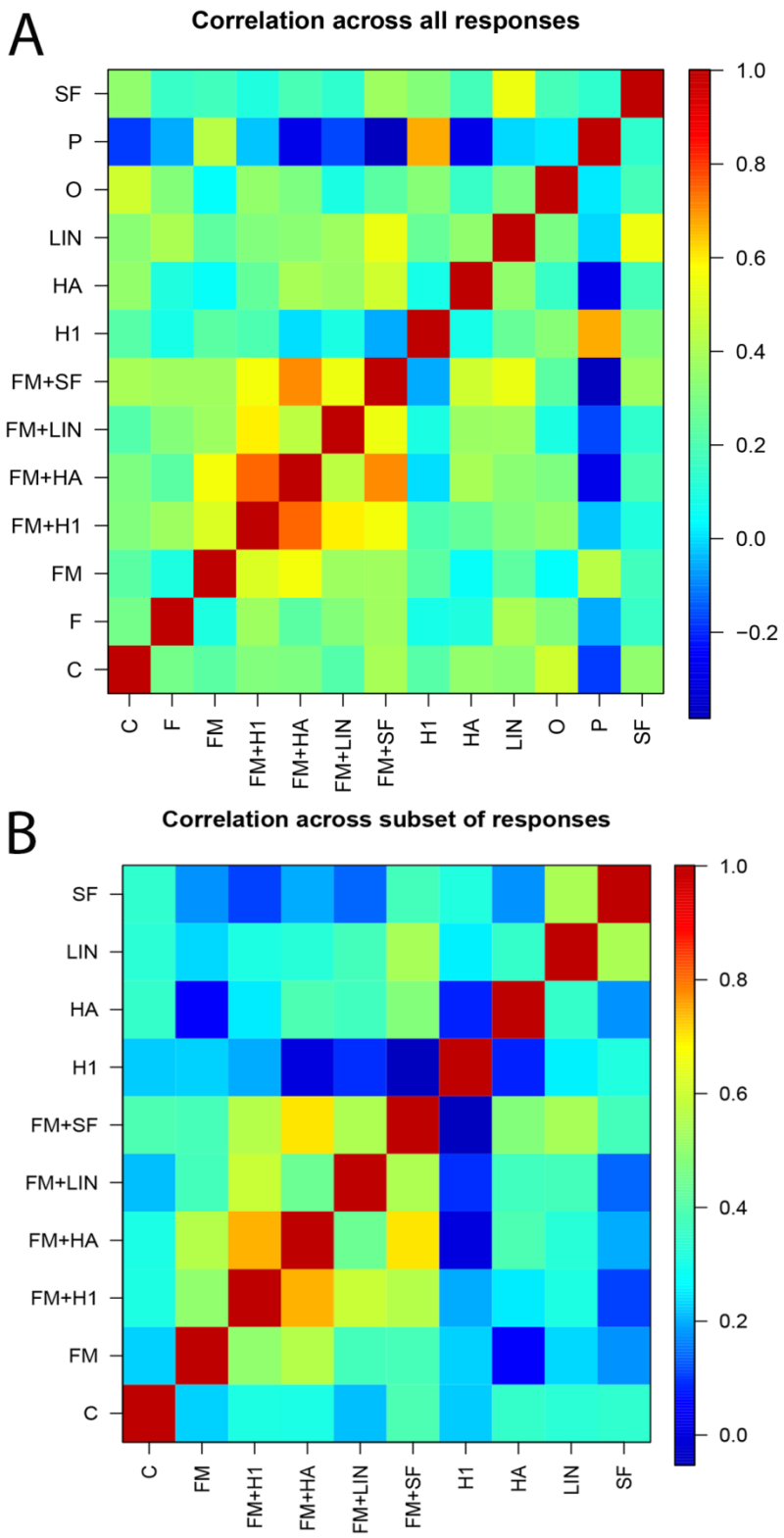

Figure 22: A. Correlation Graph showing every response, from every recordable glomeruli to all stimuli, from every recordable antennal lobe (AL), across the whole AL (Z = Z9-14-Ald, SF = Sunflower, S = Z9-16-Ald, Q = Z11-16-OH, P = Z11-16-Ald, O = Ocimene, LIN = Linalool, HA = Hexanyl acetate, H1 = Hexen-1-ol, FM = Pheromone mix, F = Farnesene, C = Control, A = Z11-16-AC). **B**. Correlation graph showing a subset from figure 6A of every response, from every recordable glomeruli to all stimuli, from every recordable AL, across the whole AL.

4. Discussion

The results of this master's project include measurement of spontaneous activity in successfully stained AL glomeruli of both moth species. Populations of PNs in the AL glomeruli were successfully stained, allowing for measurement of output signals that are conveyed along the mALT. Time traces of individual glomerular response patterns and AL maps were generated to further the analysis of the effects of antennal stimulation with the different plant odours and pheromones. It was identified that there was an overall suppressive effect in the AL when using ternary stimuli compared to the influence of single plant odours alone. As well as this, it was shown that pheromone mixture stimulation had a greater glomerular response than single pheromone components. The majority of plant odour stimuli possessed a weak correlation with each other, and there was a weak negative correlation between the primary pheromone component and all ternary mixtures. The primary pheromone component also had a moderate correlation with the pheromone mixture (FM).

4.1. *Measurements from uniglomerular medial-tract PNs*

PNs in the AL were stained using fura-dextran, via retrograde staining, to obtain recordings for output representation, with signals being recorded from the dendrites in the glomeruli. It is highly unlikely that anything other than the PNs were successfully stained and had their signals recorded due to the fura-dextran injection sites being in the calyces, which is located a great distance away from the AL. Also, the fact that the calyces are innervated mainly by uniglomerular PNs confined to the medial ALT, entails that the signals measured here belong to this distinct population of output neurons. The spontaneous activity seen in the raw data can only be as a result of successful staining of these classic uniglomerular PNs.

4.2. *Time traces*

Within the ordinary glomeruli in the AL, the same few glomeruli that consistently had the strongest responses to all stimuli, shown in figure 5 through 11, were all located within close proximity to each other. A similar kind of glomerular representation was also found by Skiri *et al* (2004) where different odorants shared an overlap of responses in the same or neighbouring glomeruli. Skiri *et al* (2004) noted that an overlap was not expected due to the characteristics of the receptor neurons showing specific responses mainly to one key compound. It should be noted, that all odours were mixed with hexane. This solvent may have contributed to the responses, as there was a small response in the same ROIs from figures 5 through 11.

The overlap may have occurred as a result of the LNs contributing with excitatory input (discussed below). In the example of glomerular response to sunflower in figure 10, there was a sharp increase followed by a sharp decrease. This could be as a result of the sunflower headspace containing many components, resulting in strong activation of LNs causing immediate suppression resulting in a sharp spike, as opposed to the gradual decrease in response as seen in responses to other stimuli. The AL maps provided a way to determine which glomeruli responded. For future work it would be useful to use the digital atlases of the antennal lobe of *H. virescens* (Berg *et al* 2002; Løfaldli et al 2010) and *H. armigera* (Zhao et al 2016) to make comparison between individuals of the same species.

It was difficult to determine whether the glomerular responses to the female produced compounds were from the MGC, as this region, being located dorsally in the AL close to the antennal nerve, was not always visible in all preparations. As a result, the ROIs that were responding the strongest may not be MGC glomeruli. A common physiological feature in all heliothine species is the arrangement of the male-specific MGC. Generally, one large centrally located unit, known as the cumulus, is found to be surrounded by either two or three smaller satellite glomeruli (four MGC units in total for *H. virescens*) (Berg *et al*, 2014). In order to segregate the MGC from the ordinary glomeruli in the examples from figure 13 through figure 17, this common physiological feature was looked for in the AL map. However, it should be noted that although the ROIs selected in figure 13 through figure 17 had the strongest responses, which may highlight them as MGC glomeruli, the AL map generated in figures 13 through 17 lacked the arrangement of the male-specific MGC. As such, it made it unclear whether these ROIs were true MGC glomeruli. Although weak, there were also responses to the female produced compounds in the part of the AL associated with the ordinary glomeruli. Similar findings have also been observed by Trona *et al* (2010), where responses to sex pheromone components were found in PNs connected to ordinary glomeruli in the male codling moth *Cydia pomonella*. Another cause for the responses described could arise from the peripheral olfactory region. It has been show in *Cydia pomonella* that a subpopulation of OSNs responded to the main pheromone component as well as pear ester (Trona *et al*, 2010). It is also possible that the responses found in both the MGC and ordinary glomeruli are as a result of the excitatory LNs described later in the discussion.

4.3. *Odour mixtures*

Many of the early mixture processing studies previously completed have been conducted on various species, such as spiny lobsters, fish, rats, and bees (Getz & Akers, 1994; Kang & Caprio, 1997; Gentilcore & Derby 1998; Duchamp & Chaput, 2003). These investigations were concerned mostly with electrophysiological recordings from single unidentified OSNs, and presented results that showed mixture specific interaction occurring at the peripheral level. The neural odour representation however, comprises the whole combinatorial pattern of receptor activation reaching the brain (Deisg *et al*, 2006). This has since led to the calcium imaging technique being used in a number of studies in the honeybee (Joerges *et al*, 1997; Galizia *et al*, 2000; Deisig *et al*, 2006) to analyse, comprehensively, mixture processing at the level of the primary olfactory centre in the AL in populations of neurons.

As noted above, calcium imaging studies have been conducted to analyse mixture processing in the AL. A large number of these studies have used ternary mixtures that are comprised of plant odour stimuli (Joerges *et al*, 1997; Galizia *et al*, 2000; Deisig *et al*, 2006; Silbering & Galizia, 2007; Piñero *et al*, 2008; Deisig *et al*, 2010; Najar-Rodriguez *et al*, 2010). However, only a small number of investigations using this imaging technique have been performed to determine the effects of pheromone mixtures combined with plant odours in the AL of moths. To the best of my knowledge this investigation is one of only a handful that has been conducted in moths.

The plant odours used in this study have been looked into, extensively, in the lab of Hanna Mustaparta, with investigations that include the physiological characterisation of OSNs tuned to plant odours in heliothine moths. These neurons have been identified via single cell recordings combined with gas chromatography, and by doing so, have determined biologically relevant odorants (Røstelien *et al*, 2005). Generally, the experiments demonstrated that the plant odour neurons are quite narrowly tuned, with high sensitivity and selectivity, responding mainly to one key compound, which can be similarly found in neurons that are responding to pheromones (Mustaparta, 2002).

4.3.1. Suppression effect of pheromones on plant odour evoked responses

Figure 19A showed the relative maximum amplitude of glomerular responses to stimuli, with the bar graph highlighting how the presence of pheromone affects the representation of plant odours in the whole AL. The analysis conducted identifies that a suppressed glomerulus response was elicited when all of the plant odours were combined with the pheromone

mixture as compared to the response to the plant odours alone. In other words, when the number of components increases within the odour mixture, there seems to be some form of active inhibition occurring within the AL. In this case it is likely coming from the MGC due to the odour mixture comprising pheromone components. This active inhibition coincides with studies conducted by Joerges *et al* (1997), Deisig *et al* (2006), Piñero *et al* (2008), Riffell *et al* (2009), and Deisig *et al* (2010), where it has been shown, when looking at the amplitude of the glomerular response to plant odour mixtures, that there were greater responses to the single odour components compared to those induced by the odour mixtures used, and that the more components used in the mixture, the greater the suppression effect.

The inhibition seen, resulting in the suppression, may be as a result of using high concentrations in the mixtures (Duchamp-Viret *et* al, 2003). Alternatively, the inhibition may come from the AL circuitry itself. The work of Distler & Boeckh (1997) showed that in the AL of cockroaches, the inhibitory LNs are able to synapse in a loop back to the presynaptic terminal on OSNs, which, in spiny lobsters and rats, results in the inhibition of electrophysiological responses of their OSNs (Deisig *et al*, 2006).

This type of global inhibition in these species is noted as a gain control which prevents the saturation of odour evoked responses, resulting in the ability to encode odours over a wider dynamic range (Deisig *et al*, 2006). Olsen & Wilson (2008) also found a similar gain control system in drosophila. It was shown that when the input from OSNs is weak, the synapses between OSNs and PNs are strong, and any lateral inhibition occurring is marginal. However, when numerous OSN input to a large number of glomeruli is recruited, the GABAergic LNs inhibit the neurotransmitter release from the OSNs, thus preventing stimulus saturation of a dynamic range of numerous PN types simultaneously (Olsen &Wilson, 2008). This type of gain control supresses strong, redundant responses, and can reduce cross correlation between output of different glomeruli, thereby promoting an efficient neural code for odours (Olsen &Wilson, 2008). The results presented in this thesis (Figure 19A) could represent a gain control mechanism.

A number of studies have reported the range of heterogeneity and homogeneity of LNs in the AL of insects (Matsumoto *et al*, 1981; Hansson *et al*, 1994; Han *et al*, 2005). Sachse and Galizia (2002) had proposed a model for the honeybee where homogeneous and heterogeneous LNs could be involved in lateral and global inhibition, with the homogeneous LNs taking part in gain control, and heterogeneous LNs taking part in lateral inhibition

between neighbouring glomeruli. This inhibitory network could trigger the suppression found in the results of figure 19A. However, it is important to note that although heterogeneous LNs have been identified in many insect species, they have not yet been found in *H. virescens*. This may be as a result of species specific functional differences in coding mechanisms, including differences in the numbers of LNs (Seki & Kanzaki *et al*, 2008). The gain control mechanism mentioned may be behaviourally relevant for the moth, as suppression of the plant odour responses when pheromones are detected would allow for the male to better track the location of the female.

4.3.2. Synergistic effect of sunflower on pheromone-evoked responses

Figure 19B shows the relative maximum amplitude of responses of glomeruli to stimuli, with the bar graph highlighting how the presence of plant odours affected the representation of pheromone signals in the whole AL. The investigation showed that the only combination that had an increased response when plant odours were added to the pheromone mixtures in the whole AL was sunflower (SF) combined with pheromone mix (FM), where there were significantly more glomeruli activated across the whole AL than during stimulation with 'FM' alone. The remaining odour mixtures produced approximately the same number of glomerular responses than 'FM' alone.

A similar synergistic effect has also been shown in electrophysiological studies by Namiki *et al* (2008) in the moth *Bombyx mori*. Other electrophysiological investigations, and combined electrophysiological and optical imaging method investigations have shown a suppressive effect, however (Chaffiol *et al*, 2012; Deisig *et al*, 2012, respectively). The synergistic effect shown in this thesis may be as a result of excitatory lateral interaction, as the MGC and the plant odour glomeruli are connected by the LNs, thus making this type of interneuron a mediator of the pheromone and plant odour interaction (Namiki *et al*, 2008). Although Seki & Kanzaki (2008) showed that the majority of the LNs within the AL of *B. mori* are GABAergic, Iwano & Kanzaki (2005) had shown in the same species, that there are also non GABAergic LNs present. This has also been shown across other species: Shang *et al* (2007) reported cholinergic excitatory LNs in the AL circuitry of drosophila, and Berg *et al* (2009) revealed, in *H. virescens*, a small number of non-GABAergic LNs containing the neuropeptide tachykinin. It is possible that the excitatory effect may also be conveyed via two synapses of the GABAergic LNs creating an overall disinhibition, which promotes an enhancement of the signal. If there are LNs that are transmitting excitatory neurotransmitter

that connects plant odour glomeruli with the MGC, the increased activity of plant odour glomeruli PNs could result in the excitation of MGC PNs (Namiki *et al*, 2008).

4.4. *Effects of pheromone mixture and single pheromone components in the MGC*

As noted above, after having completed the moth preparations, it was difficult to ascertain which of the glomerular responses to the female produced compounds were from the MGC, as the relevant region was not always visible. The arrangement of the MGC that is expected to be seen (large central cumulus surrounded by three satellite glomeruli) was looked for in all the AL maps created, after manual exclusion of irrelevant responses. From here, it was determined whether these glomeruli responded to the female produced compounds. If there was a response to the female produced compounds then, it was included in the analysis. This selection process resulted in selecting ROIs that might not be MGC glomeruli.

The results from figure 21A showed that in the pooled data of both moth species, overall, the response to pheromone mixture was greater than the response to the primary pheromone component alone. This is probably due to the chemotopic arrangement, where the male-specific OSNs project to distinct MGC glomeruli in the AL. The cumulus has been shown to process information regarding the primary pheromone component, whereas the surrounding satellite glomeruli process the information about the secondary pheromone component, as well as the interspecific signals (Berg *et al*, 2014). And so the response to the pheromone mixture was greater because it contained both the primary and secondary pheromone components, thus activating more MGC units than the primary pheromone component would have done alone. The overall significant responses in figure 21A have mostly all come from the species specific signals in *H. virescens* (figure 21C), whereas the responses to the species-specific pheromone mix in *H. armigera* (figure 21B) were almost statistically significant. This is probably due to the fact that there was clearly contamination within the responses of *H. armigera*, as there is a very strong response from hexane in the MGC. If the strong hexane response had not occurred, the results for *H. armigera* would have been statistically significant.

4.5. *Methodological considerations*

An advantage of using calcium imaging as an optical method, is the fact that the activity of populations of neurons in the MGC and plant odour glomeruli are able to be recorded simultaneously. As well as this, cellular calcium concentrations can be measured with good spatial and temporal resolution, using relatively easy experimental procedures (Galizia *et al*,

1997). However, difficulties can arise when monitoring a whole tissue due to movement artifacts, which cause a reduction in signal amplitude and signal to noise ratio, and gaining access to areas of the brain can be difficult as only the superficial layers of the brain are attainable (Galizia *et al*, 1997).

Initially, during the preparation phase, up to four moths were made ready for dye injection per day, with imaging taking place the following day. After dye injection into the calyces, all of the moths were placed into a fridge to allow the dye to reach the target areas slowly over night. Leaving the moths in a cool environment overnight, with no food, trapped in the same position, and with exoskeleton and movement artifacts removed (although coated in saline solution) is likely highly uncomfortable for the moth. This may affect the quality of calcium signals and responses acquired. As such, it was decided to prepare a moth, allowing a significant amount of time for the dye to reach the target areas (four hours), and image on the same day. This was done in order to achieve higher quality results.

Due to the number of odorants being tested (16 in total), including the test recordings (to determine the presence of spontaneous activity), and any corrections that were required to be made to the apparatus for better resolution and focus, it was common that the animal would not survive the whole testing procedure. As a result, the odorants were only able to be tested once i.e. they were not reproducible for each animal. To overcome this in the future, a set number of odorants should be used at any time in order to retrieve reproducible results within each animal.

There were incidences of contamination during this investigation at two stages. The first was during the odour preparation stage. The second was during the odour stimulation stage, where odour compounds being used were adhering to the plastic tubing connected to the air flow in the calcium imaging apparatus. To overcome this, the plastic tubing was regularly replaced. And for the odour preparation, greater care must be taken to avoid contamination. During the odour stimulation stage in the experimental procedure, odour stimulus was manually initiated. This technique is not 100% accurate, and as a result, odour stimulation does not occur at the same frame, which makes the data analysis more difficult. For future experimentation, an automated system should be implemented.

4.6. *Future considerations*

To take this investigation further, an idea would be to use complimentary methodological approaches that have been well characterised, such as intracellular recordings combined with

calcium imaging. A fluorescent calcium indicator dye can be injected into cells, via the same microelectrode used for the intracellular recordings. Thus providing simultaneous measurements to show the link between cell membrane potential and intracellular calcium concentrations (Young *et al,* 2000). As well as this, although it would be a time constraining approach, it would be worthwhile looking at different concentrations and ratios used between female produced compounds and plant odours. This is due to the observation that mixture interaction is concentration dependent (Chaffiol *et al,* 2014). It should also be possible to construct a physiological atlas of mixture evoked activity, as a result of digital atlas of the AL in male and female heliothine moths.

5. Conclusion

The results of this master's project showed that the dendritic regions, plus somata of uniglomerular PNs confined to the medial antennal-lobe tract of both moth species were successfully stained. Preparations successfully stained displayed spontaneous activity via flickering glomeruli. Time traces of stimuli responses revealed that the strongest responding glomeruli were all located within close proximity to each other and may have occurred as a result of input from LNs. An overall suppressive effect of pheromones on plant odour evoked responses in the AL was identified when using ternary stimuli. A few cases of synergistic effects of plant odours on pheromone-evoked responses were found as well. In the MGC the response to the pheromone mixture was greater than that to the primary pheromone component alone.

6. Appendix

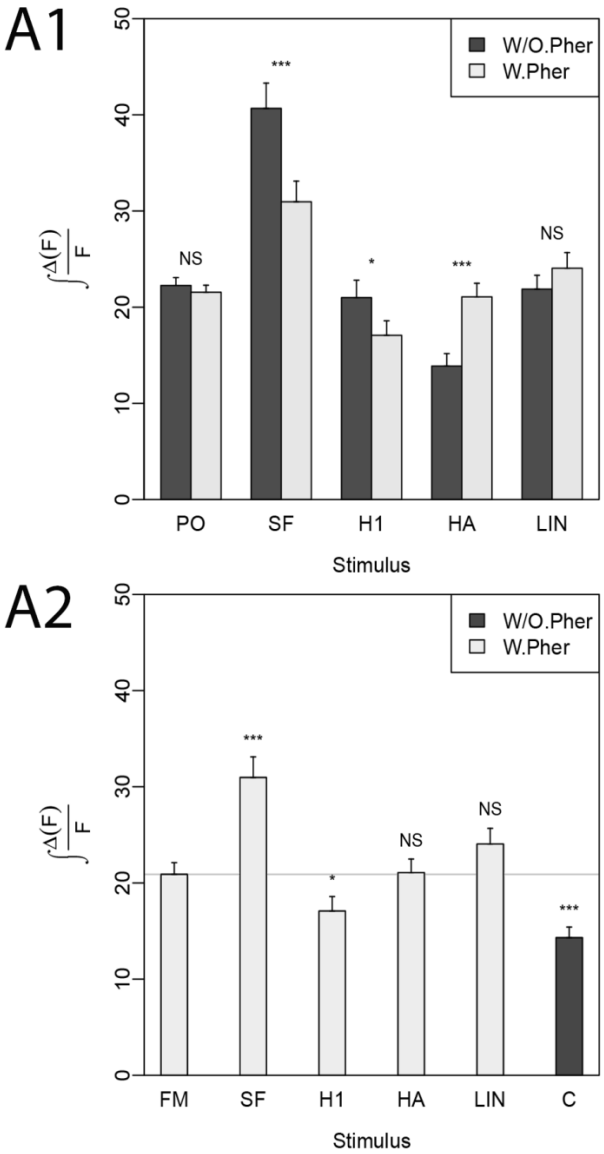

Figure A1: Bar graph representing the integral of the effects of pheromones on plant odour evoked responses. Bar graph showing the pooled data of the relative maximum response of glomeruli (measured as $\int \frac{\Delta(F)}{F}$) to different stimuli (PO = All plant odours, FM = pheromone mix, SF = Sunflower, H1 = Hexen-1-ol, HA = Hexanyl acetate, LIN = Linalool) combined with 'FM' (W.Pher) vs. Without 'FM' (W/O. Pher), to determine how the presence of pheromone affects the representation of plant odours in the whole antennal lobe (AL). Standard error means are shown with stars indicting *P*-value (* = 0.05, ** = 0.01, *** = 0.001, NS = >0.05).

Figure A2: Bar graph representing the integral of the effects of plant odours on pheromone-evoked responses. Bar graph showing the pooled data of the relative maximum response of glomeruli (measured as $\int \frac{\Delta(F)}{F}$) to different stimuli ('FM', 'SF', 'H1', 'HA', and 'LIN') combined with 'FM' Vs. 'FM' alone, to determine how adding plant odours affects the representation of pheromone signals in the whole AL. Control (C) was measured against 'FM'. Standard error means are shown with stars indicting *P*-value (* = 0.05, ** = 0.01, *** = 0.001, NS = >0.05).

7. List of abbreviations

A : Z11-16: AC
AL : antennal lobe
ALT : antennal lobe tract
AP : action potential
ASTA : A type allostatin
Ats : allototropin
C : control
CNS : central nervous system
EAG : electroantennogram
F : farnesene
FaRP : FMRFamide-related peptide
FM : pheromone mix
H1 : hexen-1-ol
HA : hexanyl acetate
iACT : inner antenna-cerebral tract
ISI : interstimulus interval
KC : Kenyon cells
lALT : lateral antennal lobe tract
LIN : linalool
LN : local interneurons
mACT : middle antenna-cerebral tract
mALT : medial antennal lobe tract
MB : mushroom bodies
MGC : macroglomerular complex
mlALT : mediolateral antennal lobe tract
O : ocimene
oACT : outer antenna-cerebral tract
OB : olfactory bulb
OBP : olfactory binding protein
OSN : olfactory sensory neuron
P : Z11-16:AL
PCA : principal component analysis
PN : projection neurons
PO : all plant odours
Q : Z11-16:OH
ROI : region of interest
S : Z9-16:AL
SCR : single cell recording
SEG : suboesophageal ganglion
SF : sunflower
TKRP : tachykinin related peptide
uPN : uniglomerular projection neuron
Z : Z9-14:AL

8. References

Ache, B. W., & Young, J. M. (2005). Olfaction: diverse species, conserved principles. *Neuron*, 48 (3), 417-430.

Almaas, T. J., & Mustaparta, H. (1990). Pheromone reception in tobacco budworm moth, Heliothis virescens. *Journal of chemical ecology*, 16 (4), 1331-1347.

Almaas, T. J., & Mustaparta, H. (1991). Heliothis virescens: response characteristics of receptor neurons in sensilla trichodea type 1 and type 2. *Journal of chemical ecology*, 17 (5), 953-972.

Baker, T. C., Cossé, A. A., Lee, S. G., Todd, J. L., Quero, C., & Vickers, N. J. (2004). A comparison of responses from olfactory receptor neurons of Heliothis subflexa and Heliothis virescens to components of their sex pheromone. *Journal of Comparative Physiology A*, 190 (2), 155-165.

Berg, B. G., & Mustaparta, H. (1995). The significance of major pheromone components and interspecific signals as expressed by receptor neurons in the oriental tobacco budworm moth, Helicoverpa assulta. *Journal of Comparative Physiology A*, 177 (6), 683-694.

Berg, B. G., Almaas, T. J., Bjaalie, J. G., & Mustaparta, H. (1998). The macroglomerular complex of the antennal lobe in the tobacco budworm moth Heliothis virescens: specified subdivision in four compartments according to information about biologically significant compounds. *Journal of comparative Physiology A*, 183 (6), 669-682.

Berg, B. G., Almaas, T. J., Bjaalie, J. G., & Mustaparta, H. (2005). Projections of male-specific receptor neurons in the antennal lobe of the oriental tobacco budworm moth, Helicoverpa assulta: A unique glomerular organization among related species. *Journal of Comparative Neurology*, 486 (3), 209-220.

Berg, B. G., Galizia, C. G., Brandt, R., & Mustaparta, H. (2002). Digital atlases of the antennal lobe in two species of tobacco budworm moths, the oriental Helicoverpa assulta (male) and the American Heliothis virescens (male and female). *Journal of Comparative Neurology*, 446 (2), 123-134.

Berg, B. G., Schachtner, J., & Homberg, U. (2009). γ-Aminobutyric acid immunostaining in the antennal lobe of the moth Heliothis virescens and its colocalization with neuropeptides. *Cell and tissue research*, 335 (3), 593-605.

Berg, B. G., Schachtner, J., Utz, S., & Homberg, U. (2007). Distribution of neuropeptides in the primary olfactory center of the heliothine moth Heliothis virescens. *Cell and tissue research*, 327 (2), 385-398.

Berg, B. G., Tumlinson, J. H., & Mustaparta, H. (1995). Chemical communication in heliothine moths. *Journal of Comparative Physiology A*, 177 (5), 527-534.

Berg, B. G., Zhao, X. C., & Wang, G. (2014). Processing of pheromone information in related species of Heliothine moths. *Insects*, 5 (4), 742-761.

Boeckh, J., & Ernst, K. D. (1987). Contribution of single unit analysis in insects to an understanding of olfactory function. *Journal of Comparative Physiology A*, 161 (4), 549-565.

Calatayud, P. A. (2014). The contribution of electrophysiology to entomology. *Entomology, Ornithology and Herpetology*, 3 (1), 1-2.

Chaffiol, A., Dupuy, F., Barrozo, R. B., Kropf, J., Renou, M., Rospars, J. P., & Anton, S. (2014). Pheromone modulates plant odor responses in the antennal lobe of a moth. *Chemical senses*, 39 (5), 451-463.

Chaffiol, A., Kropf, J., Barrozo, R. B., Gadenne, C., Rospars, J. P., & Anton, S. (2012). Plant odour stimuli reshape pheromonal representation in neurons of the antennal lobe macroglomerular complex of a male moth. *The Journal of experimental biology*, 215 (10), 1670-1680.

Cho, S., Mitchell, A., Mitter, C., Regier, J., Matthews, M., & Robertson, R. O. N. (2008). Molecular phylogenetics of heliothine moths (Lepidoptera: Noctuidae: Heliothinae), with comments on the evolution of host range and pest status. *Systematic Entomology*, 33 (4), 581-594.

Christensen, T. A., D'Alessandro, G., Lega, J., & Hildebrand, J. G. (2001). Morphometric modeling of olfactory circuits in the insect antennal lobe: I. Simulations of spiking local interneurons. *Biosystems*, 61 (2), 143-153.

Christensen, T. A., Waldrop, B. R., Harrow, I. D., & Hildebrand, J. G. (1993). Local interneurons and information processing in the olfactory glomeruli of the moth Manduca sexta. *Journal of Comparative Physiology A*, 173 (4), 385-399.

Deisig, N., Giurfa, M., & Sandoz, J. C. (2010). Antennal lobe processing increases separability of odor mixture representations in the honeybee.*Journal of neurophysiology*, 103 (4), 2185-2194.

Deisig, N., Giurfa, M., Lachnit, H., & Sandoz, J. C. (2006). Neural representation of olfactory mixtures in the honeybee antennal lobe. *European Journal of neuroscience*, 24 (4), 1161-1174.

Deisig, N., Kropf, J., Vitecek, S., Pevergne, D., Rouyar, A., Sandoz, J. C., Lucas, P., Gadenne, C., Anton, S., & Barrozo, R. (2012). Differential interactions of sex pheromone and plant odour in the olfactory pathway of a male moth. *PloS one*, 7 (3), 1-10.

Distler, P. G., & Boeckh, J. (1997). Synaptic connections between identified neuron types in the antennal lobe glomeruli of the cockroach, Periplaneta americana: II. Local multiglomerular interneurons. *Journal of Comparative Neurology*, 383 (4), 529-540.

Duchamp-Viret, P., Duchamp, A., & Chaput, M. A. (2003). Single olfactory sensory neurons simultaneously integrate the components of an odour mixture. *European Journal of Neuroscience*, 18 (10), 2690-2696.

Galizia, C. G., & Menzel, R. (2000). Odour perception in honeybees: coding information in glomerular patterns. *Current opinion in neurobiology*, 10 (4), 504-510.

Galizia, C. G., & Rössler, W. (2010). Parallel olfactory systems in insects: anatomy and function. *Annual review of entomology*, 55, 399-420.

Galizia, C. G., Joerges, J., Küttner, A., Faber, T., & Menzel, R. (1997). A semi-in-vivo preparation for optical recording of the insect brain. *Journal of neuroscience methods*, 76 (1), 61-69.

Galizia, C. G., Küttner, A., Joerges, J., & Menzel, R. (2000). Odour representation in honeybee olfactory glomeruli shows slow temporal dynamics: an optical recording study using a voltage-sensitive dye. *Journal of insect physiology*, 46 (6), 877-886.

Gentilcore, L. R., & Derby, C. D. (1998). Complex binding interactions between multicomponent mixtures and odorant receptors in the olfactory organ of the Caribbean spiny lobster Panulirus argus. *Chemical senses*, 23 (3), 269-281.

Getz, W. M., & Akers, R. P. (1994). Honeybee olfactory sensilla behave as integrated processing units. *Behavioral and neural biology*, 61 (2), 191-195.

Grienberger, C., & Konnerth, A. (2012). Imaging calcium in neurons. *Neuron*, 73 (5), 862-885.

Grynkiewicz, G., Poenie, M., & Tsien, R. Y. (1985). A new generation of Ca2+ indicators with greatly improved fluorescence properties. *Journal of Biological Chemistry*, 260 (6), 3440-3450.

Han, Q., Hansson, B. S., & Anton, S. (2005). Interactions of mechanical stimuli and sex pheromone information in antennal lobe neurons of a male moth, Spodoptera littoralis. *Journal of Comparative Physiology A*, 191 (6), 521-528.

Hansson, B. S. (2002). A bug's smell–research into insect olfaction. *Trends in neurosciences*, 25 (5), 270-274.

Hansson, B. S., & Stensmyr, M. C. (2011). Evolution of insect olfaction. *Neuron*, 72 (5), 698-711)

Hansson, B. S., Anton, S., & Christensen, T. A. (1994). Structure and function of antennal lobe neurons in the male turnip moth, Agrotis segetum (Lepidoptera: Noctuidae). *Journal of Comparative Physiology A*, 175 (5), 547-562.

Heisenberg, M. (1998). What do the mushroom bodies do for the insect brain? An introduction. *Learning & Memory*, 5 (1), 1-10.

Hillier, N. K., Kleineidam, C., & Vickers, N. J. (2006). Physiology and glomerular projections of olfactory receptor neurons on the antenna of female Heliothis virescens (Lepidoptera: Noctuidae) responsive to behaviorally relevant odors. *Journal of Comparative Physiology A*, 192 (2), 199-219.

Homberg, U., Christensen, T. A., & Hildebrand, J. G. (1989). Structure and function of the deutocerebrum in insects. *Annual review of entomology*, 34 (1), 477-501.

Ito, K., Shinomiya, K., Ito, M., Armstrong, J. D., Boyan, G., Hartenstein, V., Harzsch, S., Heisenberg, M., Homberg, U., Jenett, A., Keshishian, H., Restifo, L, L., Rössler, W., Simpson, J, H., Strausfeld N, J., Strauss, R., & Vosshall, L, B. (2014). A systematic nomenclature for the insect brain. *Neuron*, 81 (4), 755-765.

Iwano, M., & Kanzaki, R. (2005). Immunocytochemical identification of neuroactive substances in the antennal lobe of the male silkworm moth Bombyx mori. *Zoological science*, 22 (2), 199-211.

Joerges, J., Küttner, A., Galizia, C. G., & Menzel, R. (1997). Representations of odours and odour mixtures visualized in the honeybee brain. *Nature*, 387 (6630), 285-288.

Kang, J., & Caprio, J. (1997). In vivo responses of single olfactory receptor neurons of channel catfish to binary mixtures of amino acids. *Journal of neurophysiology*, 77 (1), 1-8.

Kanzaki, R., Arbas, E. A., Strausfeld, N. J., & Hildebrand, J. G. (1989). Physiology and morphology of projection neurons in the antennal lobe of the male moth Manduca sexta. *Journal of comparative Physiology A*, 165 (4), 427-453.

Kanzaki, R., Soo, K., Seki, Y., & Wada, S. (2003). Projections to higher olfactory centers from subdivisions of the antennal lobe macroglomerular complex of the male silkmoth. *Chemical senses*, 28 (2), 113-130.

Kaupp, U. B. (2010). Olfactory signalling in vertebrates and insects: differences and commonalities. *Nature Reviews Neuroscience*, 11 (3), 188-200.

Laurent, G. (2002). Olfactory network dynamics and the coding of multidimensional signals. *Nature reviews neuroscience*, 3 (11), 884-895.

Lieke, E. E. (1993). Optical recording of neuronal activity in the insect central nervous system: odorant coding by the antennal lobes of honeybees. *European Journal of Neuroscience*, 5 (1), 49-55.

Løfaldli, B. B., Kvello, P., & Mustaparta, H. (2010). Integration of the antennal lobe glomeruli and three projection neurons in the standard brain atlas of the moth Heliothis virescens. *Front. Syst. Neurosci*, 4 (5), 1-12.

Matsumoto, S. G., & Hildebrand, J. G. (1981). Olfactory mechanisms in the moth Manduca sexta: response characteristics and morphology of central neurons in the antennal lobes. *Proceedings of the Royal Society of London B: Biological Sciences*, 213 (1192), 249-277.

Mozuraitis, R., Stranden, M., Ramirez, M. I., Borg-Karlson, A. K., & Mustaparta, H. (2002). (-)-Germacrene D increases attraction and oviposition by the tobacco budworm moth Heliothis virescens. *Chemical senses*, 27 (6), 505-509.

Mustaparta, H. (1996). Central mechanisms of pheromone information processing. *Chemical senses*, 21 (2), 269-275.

Mustaparta, H. (2002). Encoding of plant odour information in insects: peripheral and central mechanisms. *Entomologia Experimentalis et Applicata*, 104 (1), 1-13.

Najar-Rodriguez, A. J., Galizia, C. G., Stierle, J., & Dorn, S. (2010). Behavioral and neurophysiological responses of an insect to changing ratios of constituents in host plant-derived volatile mixtures. *Journal of Experimental Biology*, 213 (19), 3388-3397.

Namiki, S., Iwabuchi, S., & Kanzaki, R. (2008). Representation of a mixture of pheromone and host plant odor by antennal lobe projection neurons of the silkmoth Bombyx mori. *Journal of Comparative Physiology A*, 194 (5), 501-515.

Olsen, S. R., & Wilson, R. I. (2008). Lateral presynaptic inhibition mediates gain control in an olfactory circuit. *Nature*, 452 (7190), 956-960.

Piñero, J. C., Galizia, C. G., & Dorn, S. (2008). Synergistic behavioral responses of female oriental fruit moths (Lepidoptera: Tortricidae) to synthetic host plant-derived mixtures are mirrored by odor-evoked calcium activity in their antennal lobes. *Journal of Insect Physiology*, 54 (2), 333-343.

Reisenman, C. E., Dacks, A. M., & Hildebrand, J. G. (2011). Local interneuron diversity in the primary olfactory center of the moth Manduca sexta. *Journal of Comparative Physiology A*, 197 (6), 653-665.

Riffell, J. A., Lei, H., Christensen, T. A., & Hildebrand, J. G. (2009). Characterization and coding of behaviorally significant odor mixtures. *Current Biology*, 19 (4), 335-340.

Rø, H., Müller, D., & Mustaparta, H. (2007). Anatomical organization of antennal lobe projection neurons in the moth Heliothis virescens. *Journal of Comparative Neurology*, 500 (4), 658-675.

Røstelien, T., Borg-Karlson, A. K., & Mustaparta, H. (2000). Selective receptor neurone responses to E-β-ocimene, β-myrcene, E, E-α-farnesene and homo-farnesene in the moth Heliothis virescens, identified by gas chromatography linked to electrophysiology. *Journal of Comparative Physiology A*, 186 (9), 833-847.

Røstelien, T., Borg-Karlson, A. K., Fäldt, J., Jacobsson, U., & Mustaparta, H. (2000). The plant sesquiterpene germacrene D specifically activates a major type of antennal receptor neuron of the tobacco budworm moth Heliothis virescens. *Chemical senses*, 25 (2), 141-148.

Røstelien, T., Stranden, M., Borg-Karlson, A. K., & Mustaparta, H. (2005). Olfactory receptor neurons in two heliothine moth species responding selectively to aliphatic green leaf volatiles, aromatic compounds, monoterpenes and sesquiterpenes of plant origin. *Chemical senses*, 30 (5), 443-461.

Sachse, S., & Galizia, C. G. (2002). Role of inhibition for temporal and spatial odor representation in olfactory output neurons: a calcium imaging study. *Journal of neurophysiology*, 87 (2), 1106-1117.

Sachse, S., & Krieger, P. D. J. (2011). Olfaction in insects. *E-neuroforum*, 2 (3), 49-60.

Sato, K., Pellegrino, M., Nakagawa, T., Nakagawa, T., Vosshall, L. B., & Touhara, K. (2008). Insect olfactory receptors are heteromeric ligand-gated ion channels. *Nature*, 452 (7190), 1002-1006.

Schachtner, J., Schmidt, M., & Homberg, U. (2005). Organization and evolutionary trends of primary olfactory brain centers in Tetraconata (Crustacea+ Hexapoda). *Arthropod Structure & Development*, 34 (3), 257-299.

Schmidt, C. O., Bouwmeester, H. J., de Kraker, J. W., & König, W. A. (1998). Biosynthesis of (+)-and (−)-Germacrene D in Solidago canadensis: Isolation and Characterization of Two Enantioselective Germacrene D Synthases. *Angewandte Chemie International Edition*, 37 (10), 1400-1402.

Seki, Y., & Kanzaki, R. (2008). Comprehensive morphological identification and GABA immunocytochemistry of antennal lobe local interneurons in Bombyx mori. *Journal of Comparative Neurology*, 506 (1), 93-107.

Shang, Y., Claridge-Chang, A., Sjulson, L., Pypaert, M., & Miesenböck, G. (2007). Excitatory local circuits and their implications for olfactory processing in the fly antennal lobe. *Cell*, 128 (3), 601-612.

Shepherd, G.M. 1974. *The synaptic organization of the brain. An introduction*. Oxford University Press: New York

Silbering, A. F., & Galizia, C. G. (2007). Processing of odor mixtures in the Drosophila antennal lobe reveals both global inhibition and glomerulus-specific interactions. *The Journal of Neuroscience*, 27 (44), 11966-11977.

Skiri, H. T., Galizia, C. G., & Mustaparta, H. (2004). Representation of primary plant odorants in the antennal lobe of the moth Heliothis virescens using calcium imaging. *Chemical Senses*, 29 (3), 253-267.

Steinbrecht, R. A., Laue, M., & Ziegelberger, G. (1995). Immunolocalization of pheromone-binding protein and general odorant-binding protein in olfactory sensilla of the silk moths Antheraea and Bombyx. *Cell and Tissue Research*, 282 (2), 203-217.

Stranden, M., Borg-Karlson, A. K., & Mustaparta, H. (2002). Receptor neuron discrimination of the germacrene D enantiomers in the moth Helicoverpa armigera. *Chemical senses*, 27 (2), 143-152.

Strauch, M., Rein, J., Lutz, C., & Galizia, C. G. (2013). Signal extraction from movies of honeybee brain activity: the ImageBee plugin for KNIME.*BMC bioinformatics*, 14 (18), 1-13.

Suh, E., Bohbot, J. D., & Zwiebel, L. J. (2014). Peripheral olfactory signaling in insects. *Current opinion in insect science*, 6, 86-92.

Sun, X. J., Tolbert, L. P., & Hildebrand, J. G. (1997). Synaptic organization of the uniglomerular projection neurons of the antennal lobe of the moth Manduca sexta: a laser scanning confocal and electron microscopic study.*Journal of Comparative Neurology*, 379 (1), 2-20.

Trona, F., Anfora, G., Bengtsson, M., Witzgall, P., & Ignell, R. (2010). Coding and interaction of sex pheromone and plant volatile signals in the antennal lobe of the codling moth Cydia pomonella. *The Journal of experimental biology*, 213 (24), 4291-4303.

Young, S. R., Wong, R. K., & Bianchi, R. (2000). Simultaneous intracellular recording and calcium imaging in single neurons of hippocampal slices. *Methods*, 21 (4), 373-383.

Zhao, X. C., Chen, Q. Y., Guo, P., Xie, G. Y., Tang, Q. B., Guo, X. R., & Berg, B. G. (2016). Glomerular Identification in the Antennal Lobe of the Male Moth, Helicoverpa armigera. *Journal of Comparative Neurology*.

Zhao, X. C., Kvello, P., Løfaldli, B. B., Lillevoll, S. C., Mustaparta, H., & Berg, B. G. (2014). Representation of pheromones, interspecific signals, and plant odors in higher olfactory centers; mapping physiologically identified antennal-lobe projection neurons in the male heliothine moth. *Frontiers in systems neuroscience*, 8, 1-14.